



1 **Impact of Timanian thrust systems on the late** 2 **Neoproterozoic–Phanerozoic tectonic evolution of the** 3 **Barents Sea and Svalbard**

4
5 Jean-Baptiste P. Koehl^{1,2,3,4}, Craig Magee⁵, Ingrid M. Anell⁶

6 ¹Centre for Earth Evolution and Dynamics (CEED), University of Oslo, PO Box 1028 Blindern, N-0315 Oslo,
7 Norway.

8 ²Department of Geosciences, UiT The Arctic University of Norway in Tromsø, N-9037 Tromsø, Norway.

9 ³Research Centre for Arctic Petroleum Exploration (ARCEX), UiT The Arctic University of Norway in Tromsø, N-
10 9037 Tromsø, Norway.

11 ⁴CAGE – Centre for Arctic Gas Hydrate, Environment and Climate, UiT The Arctic University of Norway in
12 Tromsø, N-9037 Tromsø, Norway.

13 ⁵School of Earth Science and Environment, University of Leeds, Leeds, LS2 9JT, United Kingdom.

14 ⁶Department of Geosciences, University of Oslo, P.O. Box 1047 Blindern, N-0316 Oslo, Norway.

15 **Correspondence:** Jean-Baptiste P. Koehl (jean-baptiste.koehl@uit.no)

16

17 **Abstract**

18 The Svalbard Archipelago is composed of three basement terranes that record a complex
19 Neoproterozoic–Phanerozoic tectonic history, including four contractional events (Grenvillian,
20 Caledonian, Ellesmerian, and Eurekan) and two episodes of collapse- to rift-related extension
21 (Devonian–Carboniferous and late Cenozoic). These three terranes are thought to have accreted
22 during the early–mid Paleozoic Caledonian and Ellesmerian orogenies. Yet recent
23 geochronological analyses show that the northwestern and southwestern terranes of Svalbard both
24 record an episode of amphibolite (–eclogite) facies metamorphism in the latest Neoproterozoic,
25 which may relate to the 650–550 Ma Timanian Orogeny identified in northwestern Russia, northern
26 Norway and the Russian Barents Sea. However, discrete Timanian structures have yet to be
27 identified in Svalbard and the Norwegian Barents Sea. Through analysis of seismic reflection, and
28 regional gravimetric and magnetic data, this study demonstrates the presence of continuous, several
29 kilometers thick, NNE-dipping, deeply buried thrust systems that extend thousands of kilometers
30 from northwestern Russia to northeastern Norway, the northern Norwegian Barents Sea, and the
31 Svalbard Archipelago. The consistency in orientation and geometry, and apparent linkage between



32 these thrust systems and those recognized as part of the Timanian Orogeny in northwestern Russia
33 and Novaya Zemlya suggests that the mapped structures are likely Timanian. If correct, these
34 findings would indicate that Svalbard's three basement terranes and the Barents Sea were accreted
35 onto northern Norway during the Timanian Orogeny and should, hence, be attached to Baltica and
36 northwestern Russia in future Neoproterozoic–early Paleozoic plate tectonics reconstructions. In
37 the Phanerozoic, the study suggests that the interpreted Timanian thrust systems represented major
38 preexisting zones of weakness that were reactivated, folded, and overprinted by (i.e., controlled the
39 formation of new) brittle faults during later tectonic events. These faults are still active at present
40 and can be linked to folding and offset of the seafloor.

41

42 **Introduction**

43 Recognizing and linking tectonic events across different terranes is critical to plate
44 reconstructions. In the latest Neoproterozoic (at ca. 650–550 Ma), portions of northwestern Russia
45 (e.g., Timan Range and Novaya Zemlya) and the Russian Barents Sea were accreted to northern
46 Baltica by top-SSW thrusting during the Timanian Orogeny (Olovyanishnikov et al., 2000;
47 Kostyuchenko et al., 2006). Discrete Timanian structures with characteristic WNW–ESE strikes
48 are sub-orthogonal to the N–S-trending Caledonian grain formed during the closure of the Iapetus
49 Ocean (Gee et al., 1994; Witt-Nilsson et al., 1998; Johansson et al., 2004; 2005). Thus far,
50 Timanian structures have only been identified in onshore–nearshore areas of northwestern Russia
51 and northeastern Norway and offshore in the Russian Barents Sea and southeasternmost Norwegian
52 Barents Sea (Barrère et al., 2009, 2011; Marellò et al., 2010; Gernigon et al., 2018; Hassaan et al.,
53 2020a, 2020b). Therefore, the nature of basement rocks in the northern and southwestern
54 Norwegian Barents Sea remains debatable. Some studies suggest a NE–SW-trending Caledonian
55 suture within the Barents Sea (Gudlaugsson et al., 1998; Gee and Teben'kov, 2004; Breivik et al.,
56 2005; Gee et al., 2008; Knudsen et al., 2019), whereas others argue for a swing into a N–S trend
57 and merging of Norway and Svalbard's Caledonides, which are expected to continue into northern
58 Greenland (Ziegler, 1988; Gernigon and Brönnér, 2012; Gernigon et al., 2014). Regardless, these
59 models solely relate basement structures in the northern and southwestern Norwegian Barents Sea
60 to the Caledonian Orogeny, implying that Laurentia and Svalbard were not involved in the
61 Timanian Orogeny and were separated from Baltica by the Iapetus Ocean in the latest



62 Neoproterozoic (Torsvik and Trench, 1991; Cawood et al., 2001; Cocks and Torsvik, 2005; Torsvik
63 et al., 2010; Merdith et al., 2021).

64 Nonetheless, geochronological data yielding Timanian ages suggest that deformation and
65 metamorphism contemporaneous of the Timanian Orogeny affected parts of the Svalbard
66 Archipelago and Laurentia and, possibly, all Arctic regions (Estrada et al., 2018; Figure 1a): (1)
67 eclogite facies metamorphism (620–540 Ma; Peucat et al., 1989; Dallmeyer et al., 1990b) and
68 eclogite facies xenoliths of mafic–intermediate granulite in Quaternary volcanic rocks are found in
69 northern Spitsbergen (648–556 Ma; Griffin et al., 2012); (2) amphibolite facies metamorphism
70 (643 ± 9 Ma; Majka et al., 2008, 2012, 2014; Mazur et al., 2009) and WNW–ESE-striking shear
71 zones like the Vimsodden–Kosibapasset Shear Zone occur in southwestern Spitsbergen (600–537
72 Ma; Manecki et al., 1998; Faehnrich et al., 2020); and (3) xenoliths of the subduction-related
73 Midtkap igneous suite in northern Greenland yield Timanian ages (628–570 Ma; Rosa et al., 2016;
74 Estrada et al., 2018). In addition, several recent studies also show the presence of NW–SE- to E–
75 W-trending basement grain in the Norwegian Barents Sea, which could possibly represent
76 Timanian fabrics and structures (Figure 1b; Barrère et al., 2009, 2011; Marello et al., 2010; Klitzke
77 et al., 2019). Following these developments, a few paleo-plate reconstructions now place Svalbard
78 together with Baltica in the latest Neoproterozoic–Paleozoic (e.g., Vernikovsky et al., 2011).

79 To test the origin of basement grain in the northern Norwegian Barents Sea and Svalbard,
80 the present study focuses on several kilometers deep structures identified on seismic data and
81 correlated using regional gravimetric and magnetic data. These newly identified structures trend
82 WNW–ESE, i.e., parallel to the Timanian structural grain in northwestern Russia and northern
83 Norway (Figure 1a–c). The structures are described and interpreted based on their geometry and
84 potential kinematic indicators, and are compared to well-known examples of Caledonian and
85 Timanian fabrics and structures elsewhere, e.g., onshore Norway (e.g., Trollfjorden–Komagelva
86 Fault Zone; Siedlecka and Siedlecki, 1967; Siedlecka, 1975), in Svalbard (e.g., Atomfjella
87 Antiform; Witt-Nilsson et al., 1998), in northwestern Russia (Central Timan Fault; Siedlecka and
88 Roberts, 1995; Olovyanishnikov et al., 2000; Kostyuchenko et al., 2006), and in the southern
89 Norwegian Barents Sea (Barrère et al., 2011; Gernigon et al., 2014) and the Russian Barents Sea
90 (Baidaratsky fault zone; Lopatin et al., 2001; Korago et al., 2004). A scenario involving several
91 episodes of deformation (Timanian Orogeny, and reactivation and overprinting during the
92 Caledonian Orogeny, Devonian–Carboniferous extension, Triassic extension, Eurekan tectonism,



93 and present-day tectonism) is proposed and the implications for the tectonic evolution of the
94 Barents Sea and the Svalbard Archipelago and associated basins (e.g., Ora and Olga basins; Anell
95 et al., 2016) are discussed.

96 Should our interpretation of discrete Timanian structures throughout the Norwegian
97 Barents Sea and Svalbard be validated, it would support accretion of these terranes to Baltica in
98 the late Neoproterozoic and place the Caledonian suture farther west than is commonly suggested
99 (e.g., Breivik et al., 2005; Gernigon et al., 2014), thus leading to a major revision of plate tectonics
100 models. In addition, constraining the extent and reactivation history of such faults may shed some
101 light on their influence on younger tectonic events, such as Caledonian, Ellesmerian and Eurekan
102 contraction, Devonian–Carboniferous collapse–rifting, and late Cenozoic breakup and ongoing
103 extension.

104

105 **Geological setting**

106 ***Timanian Orogeny***

107 The Timanian Orogeny corresponds to a ca. 650–550 Ma episode of NNE–SSW
108 contractional deformation that affected northwestern Russia and northeastern Norway. During this
109 tectonic episode, crustal-scale, WNW–ESE-striking, NNE-dipping thrusts systems with south-
110 southwestwards transport direction (top-SSW; Siedlecka and Siedlecki, 1967; Siedlecka, 1975;
111 Figure 1b), accreted portions of the Russian Barents Sea and northwestern Russia onto northeastern
112 Baltica, including Novaya Zemlya, Severnaya Zemlya, the Kanin Peninsula, the Timan Range, and
113 the Kola Peninsula (Siedlecka and Roberts, 1995; Olovyanishshnikov et al., 2000; Roberts and
114 Siedlecka, 2002; Gee and Pease, 2004; Kostyuchenko et al., 2006; Lorenz et al., 2008; Marelllo et
115 al., 2013) and the Varanger Peninsula in northeastern Norway (Siedlecka and Siedlecki, 1967;
116 Siedlecka, 1975; Roberts and Olovyanishshnikov, 2004; Herrevold et al., 2009; Drachev, 2016;
117 Figure 1a). Major Timanian thrusts include the Baidaratsky fault zone in the Russian Barents Sea
118 and Novaya Zemlya (Figure 1a–b; Eldholm and Ewing, 1971, their figure 4 profile C–D; Lopatin
119 et al., 2001; Korago et al., 2004; Drachev, 2016), the Central Timan Fault on the Kanin Peninsula
120 and the Timan Range (Siedlecka and Roberts, 1995; Olovyanishshnikov et al., 2000; Kostyuchenko
121 et al., 2006), and the Trollfjorden–Komagelva Fault Zone in northern Norway (Siedlecka and
122 Siedlecki, 1967; Siedlecka, 1975; Herrevold et al., 2009).

123



124 ***Accretion of Svalbard basement terranes in the early Paleozoic***

125 The Svalbard Archipelago consists of three Precambrian basement terranes, some of which
126 show affinities with Greenland (northwestern and northeastern terranes), whereas others are
127 possibly derived from Pearya (southwestern terrane; Harland and Wright, 1979; Ohta et al., 1989;
128 Gee and Teben'kov, 2004; Labrousse et al., 2004; Piepjohn et al., 2013; Fortey and Bruton, 2013).
129 These terranes are inferred to have accreted during the mid-Paleozoic Caledonian (collision of
130 Greenland with Svalbard and Norway at ca. 460–410 Ma; Horsfield, 1972; Dallmeyer et al., 1990a;
131 Johansson et al., 2004, 2005; Faehrich et al., 2020) and Late Devonian Ellesmerian orogenies
132 (Piepjohn, 2000; Majka and Kosminska, 2017). In these models, accretion was facilitated via
133 hundreds of kilometers of displacement along (arcuate) strike-slip faults, such as the Billefjorden
134 Fault Zone (Harland, 1969; Harland et al., 1992; Labrousse et al., 2008) and the Lomfjorden Fault
135 Zone (Piepjohn et al., 2019; Figure 2), although other studies suggest more limited strike-slip
136 displacement (Lamar et al., 1986; Manby and Lyberis, 1992; Manby et al., 1994; Lamar and
137 Douglass, 1995). These large (strike-slip?) faults are assumed to have extended thousands of
138 kilometers southwards and to represent the continuation of Caledonian faults in Scotland (Norton
139 et al., 1987; Dewey and Strachan, 2003). Caledonian contraction resulted in the formation of large
140 fold and thrust complexes, such as the Atomfjella Antiform in northeastern Spitsbergen (Gee et al.,
141 1994; Witt-Nilsson et al., 1998) and the Rijpdalen Anticline in Nordaustlandet (Johansson et al.,
142 2004; 2005; Dumais and Brönnér, 2020), whereas Ellesmerian tectonism is thought to have formed
143 narrow fold and thrust belts, like the Dickson Land and Germaniahavøya fold-thrust zones
144 (McCann, 2000; Piepjohn, 2000; Dallmann and Piepjohn, 2020).

145 In northern Norway, Timanian thrusts were reactivated–overprinted in subsequent tectonic
146 events (e.g., Caledonian Orogeny and late–post-Caledonian collapse–rifting) as dominantly strike-
147 to oblique-slip faults (Siedlecka and Siedlecki, 1971; Roberts et al., 1991; Herrevold et al., 2009;
148 Rice, 2014). A notable example is the folding and reactivation of Timanian fabrics and structures
149 (e.g., Trollfjorden–Komagelva Fault Zone) during the Caledonian Orogeny (Siedlecka and
150 Siedlecki, 1971; Herrevold et al., 2009) and intrusion of Mississippian dolerite dykes along steeply
151 dipping WNW–ESE-striking brittle faults that overprint the Trollfjorden–Komagelva Fault Zone
152 onshore–nearshore northern Norway (Roberts et al., 1991; Lippard and Prestvik, 1997; Nasuti et
153 al., 2015; Koehl et al., 2019).

154



155 ***Late Paleozoic post-Caledonian collapse and rifting***

156 In the latest Silurian–Devonian, extensional collapse of the Caledonides led to the
157 deposition of several kilometers thick sedimentary basins such as the Devonian Graben in northern
158 Spitsbergen (Gee and Moody-Stuart, 1966; Friend et al., 1966; Friend and Moody-Stuart, 1972;
159 Murascov and Mokin, 1979; Manby and Lyberis, 1992; Manby et al., 1994; Friend et al., 1997;
160 McCann, 2000; Dallmann and Piepjohn, 2020). In places, N–S-trending basement ridges
161 potentially exhumed as metamorphic core complexes along bowed, reactivated detachments, such
162 as the Keisarhjelmen Detachment in northwestern Spitsbergen (Braathen et al., 2018).

163 In the latest Devonian–Mississippian, coal-rich sedimentary strata of the Billefjorden
164 Group were deposited within normal fault-bounded basins throughout Spitsbergen (Cutbill and
165 Challinor, 1965; Harland et al., 1974; Cutbill et al., 1976; Aakvik, 1981; Koehl and Muñoz-Barrera,
166 2018; Koehl, 2020a) and the Norwegian Barents Sea (Koehl et al., 2018a; Tonstad, 2018). As rift-
167 related normal faulting evolved, Pennsylvanian sedimentation was localized into a few, several
168 kilometers deep, N–S-trending basins like the Billefjorden Trough (Cutbill and Challinor, 1965;
169 Braathen et al., 2011; Koehl et al., 2021 in review) and the Ora Basin (Anell et al., 2016). In the
170 Permian, rift-related faulting stopped and platform carbonates were deposited throughout Svalbard
171 (Cutbill and Challinor, 1965) and the Barents Sea (Larssen et al., 2005).

172 Overall, the several kilometers thick, late Paleozoic sedimentary succession deposited
173 during late–post-Caledonian extension buried Proterozoic basement rocks. As a result, these rocks
174 are sparsely exposed and, thus, difficult to study.

175

176 ***Mesozoic sedimentation and magmatism***

177 In the Mesozoic, Svalbard and the Barents Sea remained tectonically quiet and were only
178 affected by minor Triassic normal faulting (e.g., Anell et al., 2013; Osmundsen et al., 2014; Ogata
179 et al., 2018; Smyrak-Sikora et al., 2020). In the Early Cretaceous, Svalbard was affected by a
180 regional episode of magmatism recorded by the intrusion of numerous dykes and sills of the
181 Diabasodden Suite (Senger et al., 2013).

182

183 ***Early Cenozoic Eurekan tectonism***

184 The opening of the Labrador Sea and Baffin Bay between Greenland and Arctic Canada in
185 the early Cenozoic (Chalmers and Pulvercraft, 2001; Oakey and Chalmers, 2012) led to the



186 collision of northern Greenland with Svalbard and the formation of a fold-and-thrust belt with top-
187 east thrusts and east-verging folds in western Spitsbergen (Dallmann et al., 1993). In eastern
188 Spitsbergen, this deformation event is characterized by dominantly thin-skinned deformation
189 structures, including décollements, some of which showing westwards transport directions
190 (Andresen et al., 1992; Haremo and Andresen, 1992). Notably, the N–S-striking Agardhbukta
191 Fault, a major splay/segment of the Lomfjorden Fault Zone, accommodated reverse and, possibly,
192 strike-slip movements during this event (Piepjohn et al., 2019).

193

194 *Late Cenozoic opening of the Fram Strait*

195 After the end of extension in the Labrador Sea and Baffin Bay, the Fram Strait started to
196 open in the earliest Oligocene (Engen et al., 2008). Tectonic extension and break-up in the Fram
197 Strait resulted in the formation of two major, NW–SE-striking transform faults (Lowell, 1972;
198 Thiede et al., 1990; Figure 1b).

199

200 **Methods and datasets**

201 Seismic surveys from the DISKOS database (see Figure 1b–c and supplement S1 for
202 location) were used to interpret basement-seated structures and related, younger, brittle overprints
203 (Figure 3a–f and Figure 4a–h and supplement S2). Other features of interest include potential
204 dykes, which commonly appear as high positive reflections on seismic data. The geology
205 interpreted from onshore seismic data was directly correlated to geological maps of the Norwegian
206 Polar Institute (e.g., Dallmann, 2015). Where possible, interpretation of offshore seismic data was
207 tied to onshore geological maps and to exploration wells Raddedalen-1 and Plurdalen-1 on
208 Edgeøya (Bro and Shvarts, 1983; Harland and Kelly, 1997) and to the Hopen-2 well on Hopen
209 (Anell et al., 2014; Figure 1c and supplement S3). The Raddedalen-1 well penetrated 2823 meters
210 of Upper Permian to Mississippian or Ordovician strata, the Plurdalen well 2351 meters of Middle
211 Triassic to (pre-?) Devonian strata, and the Hopen-2 well 2840 meters of Middle–Upper Triassic
212 to Pennsylvanian strata (Bro and Shvarts, 1983; Harland and Kelly, 1997; Anell et al., 2014; Senger
213 et al., 2019). Note that the interpretation of lower Paleozoic (Ordovician–Silurian) rocks in the
214 Raddedalen-1 well by Bro and Shvarts (1983) is preferred to that of upper Paleozoic (Upper
215 Devonian–Mississippian) by Cambridge Svalbard Exploration (see contrasting interpretations in
216 Harland and Kelly, 1997). This is based on the more detailed lithological, palynological and



217 paleontological analyses by the former, and on the strong contrast of the lithologies described in
218 the well with Devonian–Mississippian successions on Svalbard (Cutbill and Challinor, 1965;
219 Cutbill et al., 1976; Friend et al., 1997; Dallmann and Piepjohn, 2020).

220 Only a few examples of seismic sections are included in the present contribution. However,
221 more interpreted and uninterpreted seismic data are available as supplements (supplements S1–2).
222 None of the seismic sections were depth-converted, and the thickness are therefore discussed in
223 seconds (Two-Way Time; TWT). However, local time conversion was performed to tie seismic
224 wells onshore Edgeøya to seismic section in Storfjorden and depth conversion was performed
225 locally to evaluate fault displacement. Velocities of Gernigon et al. (2018) were used in these
226 conversions. Details related to these conversions are shown in supplement S3.

227 The correlation of kilometer-thick structures discussed in the present contribution was also
228 tested using gravimetric and magnetic data in cross section (Figure 3a–f) and regional magnetic
229 and gravimetric data in the northern Norwegian Barents Sea and Svalbard (Figure 5 and supplement
230 S4) from the Federal Institute for Geosciences and Natural Resources in Germany in map view
231 (Klitzke et al., 2019). Regional gravimetric and magnetic data are also used to interpret deep
232 basement fabrics and structures, e.g., regional folds (gravimetric highs commonly associated with
233 major anticlines of thickened dense basement (i.e., Precambrian) rocks and gravimetric lows with
234 synclines with less dense sedimentary basins) and large faults that commonly correlate with
235 elongated gravimetric and/or magnetic anomalies (e.g., Koehl et al., 2019), and to discuss the
236 relationship of the described structures with known structural trends in onshore basement rocks in
237 Russia, Norway and Svalbard.

238

239 **Results and interpretations**

240 First, the interpretation of seismic data are described by area, including (1) Storfjorden
241 (between Edgeøya and Spitsbergen) and the northeastern part of the Norwegian Barents Sea (east
242 of Edgeøya), (2) Nordmannsfonna to Sassenfjorden onshore–nearshore the eastern–central part of
243 Spitsbergen, and (3) the northwestern part of the Norwegian Barents Sea between Bjørnøya and
244 Spitsbergen (Figure 1b–c). Description in each area starts with deep Precambrian basement rocks
245 and shallow sedimentary rock units, and ends with deep brittle–ductile structures and with shallow
246 brittle faults. Then, potential field data and regional gravimetric and magnetic anomalies in the
247 Barents Sea and Svalbard are described, and compared and correlated to seismic data and to major



248 Timanian and Caledonian fabrics and structures onshore northwestern Russia, Svalbard and
249 Norway. Please see high resolution versions of all the figures and supplements on DataverseNO
250 (doi.org/10.18710/CE8ROH).

251

252 ***Structures in the northwestern–northeastern Norwegian Barents Sea, Storfjorden and central–***
253 ***eastern Spitsbergen***

254 *Storfjorden and northeastern Norwegian Barents Sea*

255 Folded Precambrian–lower Paleozoic basement rocks

256 Seismic facies at depths of 2–6 seconds (TWT) typically comprise successions of laterally
257 discontinuous (< three kilometers long), sub-horizontal, moderately curving–undulating,
258 moderate–high-amplitude seismic reflections that alternate with packages of highly-disrupted
259 and/or curved low-amplitude seismic reflections (see yellow lines within pink and purple units in
260 Figure 3a and Figure 4a). The curving geometries of the moderate–high amplitude reflections
261 display a typical kilometer- to hundreds of meter-scale wavelength and are commonly asymmetric,
262 seemingly leaning/verging towards the south/SSW (see yellow lines in Figure 4b). Based on ties
263 with well bores on Edgeøya (Raddedalen-1 well; Bro and Shvarts, 1983; Harland and Kelly, 1997),
264 these asymmetric, undulate features most likely correspond to SSW-verging folds in Precambrian–
265 lower Paleozoic basement rocks. In places, apparent reverse offsets of these undulate reflections
266 align along moderately–gently north- to NNE-dipping surfaces (see red lines in Figure 4a and c),
267 which are therefore interpreted as minor, top-south/SSW, brittle thrusts.

268 Upper Paleozoic–Mesozoic sedimentary successions

269 In Storfjorden and the northwestern Norwegian Barents Sea, shallow (0–3 seconds TWT)
270 seismic reflections above folded and thrust Precambrian–lower Paleozoic basement rocks show
271 significantly more continuous patterns (>> five kilometers), gently curving–undulating geometries
272 and only local disruptions by shallow, dominantly NNE-dipping, high-angle listric disruptions (see
273 yellow lines within orange unit in Figure 3a and c). In the northeastern Barents Sea, these
274 reflections are largely flat-lying (see yellow lines within orange unit in Figure 3b and d). Based on
275 field mapping campaigns and well-bores in adjacent onshore areas of Spitsbergen, Edgeøya, Hopen
276 and Bjørnøya (see location in Figure 1b), these continuous reflections are interpreted as mildly
277 folded upper Paleozoic–Mesozoic (–Cenozoic?) sedimentary strata (Dallmann and Krasil'scikov,
278 1996; Harland and Kelly, 1997; Worsley et al., 2001; Dallmann, 2015). The Permian–Triassic



279 boundary was correlated throughout the northern Norwegian Barents Sea and Storfjorden by using
280 the tie of Anell et al. (2014) to the Hopen-2 well.

281 Deep thrust systems

282 The packages of sub-horizontal, moderately curving–undulating (folded Precambrian–
283 lower Paleozoic basement) reflections alternate laterally from north to south with 20–60 kilometers
284 wide, up to four seconds thick (TWT), upwards-thickening, wedge-shaped packages (areas with
285 high concentrations of black lines in Figure 3a and d). These wide upwards-thickening packages
286 consist of two types of reflections. First, they include planar, continuous, gently–moderately north-
287 to NNE-dipping, sub-parallel, high-amplitude reflections that commonly merge together
288 downwards and that can be traced and correlated on several seismic sections in Storfjorden (black
289 lines in Figure 3a). Upwards, these reflections terminate against high-amplitude convex-upwards
290 reflections interpreted as intra- Precambrian–lower Paleozoic basement reflections (fuchsia lines
291 in Figure 3a and c) or continue as moderately NNE-dipping disruption surfaces that offset these
292 intra-basement reflections top-SSW (e.g., offset intra-Precambrian unconformities in Figure 3a and
293 c and Figure 4d).

294 Second, sub-parallel, high-amplitude reflections bound wedge-shaped, upwards-thickening
295 packages of asymmetric, curved, south- to SSW-leaning, moderately north- to NNE-dipping,
296 moderate-amplitude reflections showing narrow (< one kilometer wide) upwards-convex
297 geometries (Figure 4d). These asymmetric reflections also commonly appear as gently north- to
298 NNE-dipping packages of Z-shaped reflections bounded by sub-parallel, planar, high-amplitude
299 reflections (see yellow lines in Figure 4e). Asymmetric, south- to SSW-leaning, convex-upwards
300 reflections are interpreted as south- to SSW-verging fold anticlines reflecting relatively low
301 amounts of plastic deformation of layered rocks.

302 The alternation of packages of layered rocks folded into SSW-verging folds (yellow lines
303 in Figure 3a–c) with packages of planar, NNE-dipping, sub-parallel, high-amplitude reflections
304 (black lines in Figure 3a–c) suggest that the latter reflection packages represent zones where initial
305 layering was destroyed and/or possibly reoriented, i.e., areas that accommodated larger amounts of
306 deformation and tectonic displacement. Thus, planar, gently–moderately north- to NNE-dipping,
307 high-amplitude reflections (black lines in Figure 3a–c) are interpreted as low-angle brittle–ductile
308 thrust systems. We name these thrust systems (from north to south) the Steiløya–Krylen,



309 Kongsfjorden–Cowanodden, Bellsundbanken, and Kinnhøgda–Daudbjørnpynten fault zones
310 (Figure 3a and supplement S2a–b; see Figure 1c for location of the thrusts).

311 The relatively high-amplitude character of planar, NNE-dipping reflections within the
312 thrusts suggest that these tectonic structures consist of sub-parallel layers of rocks and minerals
313 with significantly different physical properties. A probable explanation for such laterally
314 continuous and consistently high-amplitude reflections is partial recrystallization of rocks layers–
315 mineral bands into rocks and minerals with significantly higher density along intra-thrust planes
316 that accommodated large amounts of displacement (e.g., mylonitization; Fountain et al., 1984;
317 Hurich et al., 1985). In places, packages of aggregates of Z-shaped reflections bounded upwards
318 and downwards by individual low-angle thrust surfaces are interpreted as forward-dipping duplex
319 structures (e.g., Boyer and Elliott, 1982) reflecting relatively strong plastic deformation between
320 low-angle, brittle–ductile (mylonitic?) thrusts (see yellow lines in Figure 4e).

321 The Kongsfjorden–Cowanodden, Bellsundbanken, and Kinnhøgda–Daudbjørnpynten fault
322 zones can be traced east-southeast of Edgeøya as a similar series of 20–60 kilometers wide, up to
323 four seconds thick (TWT), upwards-thickening packages (e.g., black lines in Figure 3d and
324 supplements S2a). However, their imaging along NNW–SSE-trending seismic sections is much
325 more chaotic and it is more difficult to identify smaller structures (like south-verging folds and
326 minor thrusts) within each thrust system (e.g., supplement S2a). This suggests that these three thrust
327 systems strike oblique to NNW–SSE-trending seismic sections (supplement S2a), whereas they are
328 most likely sub-orthogonal to N–S- to NNE–SSW-trending seismic sections in Storfjorden (Figure
329 3a). The only orientation that reconciles these seismic facies variations (i.e., well-imaged on NNE–
330 SSW-trending seismic sections and poorly imaged by NNW–SSE-trending seismic sections;
331 Figure 3a and supplement S2a) is an overall WNW–ESE strike.

332 South of each 20–60 kilometers wide packages of thrust surfaces and related fold and
333 duplex structures, seismic reflections representing Precambrian–lower Paleozoic basement rocks
334 typically appear as gently curved, convex-upwards, relatively continuous reflections showing sub-
335 horizontal seismic onlaps (see white arrows in Figure 3a–f). This suggests that Precambrian–lower
336 Paleozoic basement rocks most likely consist (meta-) sedimentary rocks (analogous to those
337 observed in northeastern Spitsbergen and Nordaustlandet; Harland et al., 1993; Stouge et al., 2011)
338 that were deposited in foreland and piggy-back basins ahead of each 20–60 kilometers wide
339 packages (Figure 3a–f).



340 Hence, based on the upwards-thickening geometry of the packages of south- to SSW-
341 verging folds and of forward-dipping duplexes, on the top-SSW reverse offsets of intra-basement
342 reflections by low-angle brittle–ductile thrust surfaces, on the upwards truncation of these low-
343 angle thrusts by intra-basement reflections, and on the onlapping geometries of (meta-)
344 sedimentary basement rocks south of each set of top-SSW thrust surfaces, the 20–60 kilometers
345 wide, upwards-thickening, wedge-shaped packages are interpreted as crustal-scale, several
346 kilometers thick, north- to NNE-dipping, top-SSW, brittle–ductile thrust systems (see fault zones
347 with high concentration of black lines in Figure 3a–f). These thrust systems include low-angle,
348 brittle–ductile, mylonitic thrust surfaces (black lines in Figure 4d–e) separating upwards-
349 thickening thrust sheets that consist of gently to strongly folded basement rocks and forward-
350 dipping duplex structures (yellow lines in Figure 4d–e). These thrust sheets are interpreted to reflect
351 accretion and stacking from the north or north-northeast. The interpreted thrust systems are
352 comparable in seismic facies and thickness to kilometer-thick mylonitic shear zones in the
353 Norwegian North Sea (Phillips et al. 2016) and southwestern Norwegian Barents Sea (Koehl et al.,
354 2018).

355 N–S-trending folds

356 On E–W seismic cross sections, reflections of the Kongsfjorden–Cowanodden,
357 Bellsundbanken, and Kinnhøgda–Daudbjørnpynten fault zones define large, 50–100 kilometers
358 wide, U-shaped, symmetrical depressions (black lines in Figure 3b) on the edge of which they are
359 truncated at a high angle and overlain by folded lower Paleozoic and mildly folded to flat-lying
360 upper Paleozoic (meta-) sedimentary rocks (purple and orange units with associated yellow lines
361 in Figure 3b). In addition, within these U-shaped depressions, the thrust systems show curving up
362 and down, symmetrical geometries with 5–15 kilometers wavelength (yellow lines within the pink
363 unit in Figure 3b and Figure 4f). Also notice the kilometer- to hundreds of meter-scale undulating
364 pattern of 5–15 kilometers wide curved geometries (yellow lines in Figure 4f). Based on the
365 truncation and abrupt upward disappearance of high-amplitude seismic reflections characterizing
366 the thrust systems, the high-angle truncation of the thrusts is interpreted as a major erosional
367 unconformity (dark blue line in Figure 3b and pink line in Figure 4f), and the large U-shaped
368 depressions as large N–S- to NNE–SSW-trending, upright regional folds (black lines in Figure 3b).
369 Furthermore, the 5–15 kilometers wide, symmetrical, curved geometries and associated, kilometer-
370 to hundreds of meter-scale, undulating pattern of seismic reflections within the thrusts are



371 interpreted as similarly (N–S- to NNE–SSW-) trending, upright, parasitic macro- to meso-scale
372 folds (yellow lines in Figure 3b and Figure 4f).

373 Shallow brittle faults

374 In places, near the top of the 20–60 kilometers wide thrust systems (Kongsfjorden–
375 Cowanodden, Bellsundbanken, and Kinnhøgda–Daudbjørnpynten fault zones), low-angle brittle–
376 ductile thrust surfaces merge upwards with high-angle to vertical, listric, north- to NNE-dipping
377 disruption surfaces at depths of c. 2–3 seconds (TWT; see red lines in Figure 3a and d). These
378 listric disruption surfaces truncate shallow, laterally continuous reflections that display gently
379 curved, symmetric geometries in Storfjorden (yellow lines in Figure 3a) and flat-lying geometries
380 in the northeastern Norwegian Barents Sea (yellow lines in Figure 3d). Notably, they show minor,
381 down-NNE normal offsets, and related minor southwards thickening (towards the disruption) of
382 seismic sub-units within Devonian–Carboniferous (–Permian?) sedimentary strata in the north,
383 both in Storfjorden and the northeastern Barents Sea (Figure 3a–d and white double arrows in
384 Figure 4g). In addition, they display minor reverse offsets and associated gentle upright folding of
385 shallow continuous reflections potentially representing upper Mesozoic (–Cenozoic?) sedimentary
386 deposits in Storfjorden (Figure 3a–c and e, and orange lines in Figure 4h). Note that flat-lying
387 Mesozoic (–Cenozoic?) sedimentary rocks are not offset in the northeastern Norwegian Barents
388 Sea (Figure 3d).

389 Based on the observed normal offsets and southwards-thickening of Devonian–
390 Carboniferous (–Permian?) sedimentary strata north of these disruption surfaces (e.g., white double
391 arrows in Figure 4g), these are interpreted as syn-sedimentary Devonian–Carboniferous normal
392 faults. The minor reverse offsets and associated gentle upright folding of Mesozoic (–Cenozoic?)
393 sedimentary rocks in Storfjorden (e.g., orange lines in Figure 4h) suggest that these normal faults
394 were mildly inverted near Svalbard in the Cenozoic. However, it is unclear whether inversion in
395 Storfjorden initiated in the early Cenozoic or later. Nonetheless, minor reverse offset and folding
396 of the seafloor clearly indicate ongoing inversion along these faults (Figure 3a and c, and Figure
397 4h). Furthermore, considering the merging relationship between these high-angle listric disruption
398 surfaces and underlying shear zones (i.e., merging black and red lines in Figure 3a and c–d), we
399 propose that the formation of Devonian–Carboniferous normal faults was controlled by the crustal-
400 scale, north- to NNE-dipping (inherited) thrust systems (Kongsfjorden–Cowanodden,
401 Bellsundbanken, and Kinnhøgda–Daudbjørnpynten fault zones).



402

403 *Nordmannsfunna–Sassenfjorden (eastern–central Spitsbergen)*

404 Deep thrust system and N–S-trending folds

405 Seismic data from Nordmannsfunna to Sassenfjorden in eastern Spitsbergen (see Figure 1c
406 for location) show reflection packages including both planar, continuous, moderately-dipping high-
407 amplitude reflections and upwards-curving, moderate-amplitude reflections (black and yellow
408 lines in Figure 3e–f). These two sets are similar to reflection packages interpreted as low-angle,
409 brittle–ductile mylonitic thrusts bounding packages of south- to SSW-verging folds in Storfjorden
410 and the northeastern Norwegian Barents Sea (black and yellow lines in Figure 3a and d, and
411 supplement S2a). In addition, they are located at similar depths (> 2 seconds TWT) and seem to
412 align with the Kongsfjorden–Cowanodden fault zone in Storfjorden along a WNW–ESE-trending
413 axis. Hence, we interpret the deep, continuous, high-amplitude reflections in eastern Spitsbergen
414 as the western continuation of the top-SSW Kongsfjorden–Cowanodden fault zone. This thrust can
415 be traced on seismic data as gently NNE-dipping, high-amplitude reflections in Sassendalen and
416 Sassenfjorden–Tempelfjorden (supplement S2c–d), and possibly in Billefjorden (Koehl et al., 2021
417 in review, their figure 9a–b).

418 In Nordmannsfunna, the Kongsfjorden–Cowanodden fault zone (black lines in Figure 3e–
419 f) is truncated upwards by the base-Pennsylvanian unconformity (white line in Figure 3e–f; tied to
420 onshore geological maps; Dallmann, 2015) and shows pronounced variations in dip direction,
421 ranging from east-dipping in the east to NNE-dipping in the north and WNW-dipping in the west,
422 which result into a c. 15–20 kilometers wide, north- to NNE-plunging dome-shaped/convex-
423 upwards geometry (black lines in Figure 3e–f). This portion of the thrust system is interpreted to
424 be folded into a major NNE- to north-plunging upright fold, whose 3D geometry was accurately
425 constrained due to good seismic coverage in this area (Figure 1c).

426 Small-scale structures within the Kongsfjorden–Cowanodden fault zone also show
427 asymmetric folds and internal seismic units terminating upwards with convex-upwards reflections
428 (yellow lines in Figure 3e–f) suggesting top-SSW nappe thrusting in the northern portion of the
429 thrust system. However, on E–W cross sections, seismic data reveal a set of west-verging folds in
430 the east and a more chaotic pattern of symmetrical, dominantly upright folds in the west (yellow
431 lines in Figure 3e) and below a major, high-angle, east-dipping disruption surface (thick red line in
432 Figure 3e) that crosscuts the Kongsfjorden–Cowanodden fault zone.



433 Shallow brittle faults

434 The high-angle, east-dipping disruption surface (thick red line in Figure 3e) is associated
435 with minor subvertical to steeply east-dipping disruption surfaces (thin red lines in Figure 3e). This
436 feature shows a major reverse, top-west offset (> 0.5 second TWT) of seismic units and reflections
437 at depth > 0.75 second (TWT; e.g., black lines in Figure 3e), and minor reverse offset (< 0.1 second
438 TWT) and upwards-convex curving of adjacent reflections at depth < 0.75 second (TWT; white
439 line and yellow lines within blue and units in Figure 3e). Since the major disruption coincides with
440 the location of the Agardhbukta Fault (Piepjohn et al., 2019; see Figure 1 for location) and shows
441 a steep inclination near the surface similar to that of the Agardhbukta Fault, it is interpreted as the
442 subsurface expression of this fault. The Agardhbukta Fault offsets the Kongsfjorden–Cowanodden
443 fault zone in a reverse fashion (> 0.5 second TWT; black lines in Figure 3e), and terminates upwards
444 within and slightly offsets upper Paleozoic–Mesozoic sedimentary rocks (blue and black units and
445 associated yellow lines in Figure 3e), which were correlated to onshore outcrops in eastern
446 Spitsbergen (Andresen et al., 1992; Haremo and Andresen, 1992; Dallmann, 2015). As a result,
447 these rocks are folded into a N–S-trending, open, upright fold around the fault tip, both of which
448 suggest top-west movements along the fault (Figure 3e).

449 Pre-Pennsylvanian dykes

450 In the hanging wall and on the eastern flank of the folded Kongsfjorden–Cowanodden fault
451 zone in Nordmannsfunna, high- to low-amplitude, gently east-dipping seismic reflections, which
452 possibly represent sedimentary strata (light orange unit in Figure 3e), are crosscut but not offset by
453 moderately west-dipping, high-amplitude planar reflections (blue lines in Figure 3e). In NNE–
454 SSW-trending cross-sections, these high-amplitude, cross-cutting seismic reflections appear sub-
455 horizontal (blue lines in Figure 3f). These crosscutting, west-dipping reflections are mildly folded
456 in places and either terminate upwards within the suggested, gently east-dipping, sedimentary strata
457 (light orange unit in Figure 3e) or are truncated by the base-Pennsylvanian unconformity (white
458 line in Figure 3e). Downwards within the Kongsfjorden–Cowanodden fault zone (black lines in
459 Figure 3e), these inclined reflections can be vaguely traced as a series of discontinuous, subtle
460 features (see blue lines in Figure 3e). In the footwall of the Kongsfjorden–Cowanodden fault zone,
461 the inclined reflections become more prominent again, still do not offset background reflections,
462 and extend to depths of 3–3.5 seconds (TWT; blue lines in Figure 3e). The high amplitude of these
463 planar west-dipping reflections, the absence of offset across them, and their discontinuous



464 geometries across the Agardhbukta Fault and the Kongsfjorden–Cowanodden fault zone suggest
465 that they may represent dykes (see Phillips et al., 2018). Because they appear truncated by the Base-
466 Pennsylvanian unconformity, we suggest such dykes were emplaced prior to development of this
467 unconformity. The Kongsfjorden–Cowanodden fault zone is folded into a broad, 15–20 kilometers
468 wide anticline, and offset > 0.5 second (TWT) by the Agardhbukta Fault, whereas the west-dipping
469 dykes (blue lines in Figure 3e) and the gently east-dipping sedimentary strata they intrude (light
470 orange unit in Figure 3e) are only mildly folded and show no offset across the Agardhbukta Fault
471 (Figure 3e). These differences in deformation suggest that the latter were deformed during a mild
472 episode of late contraction but not by the same early episode of intense contraction that resulted in
473 macrofolding of the Kongsfjorden–Cowanodden fault zone.

474 Cretaceous dykes and sills

475 Near or at the surface, thin, kilometer-wide, lenticular packages of gently dipping,
476 moderate–high-amplitude seismic reflections (black units in Figure 3e–f) correlate with surface
477 outcrops of Cretaceous sills of the Diabasodden Suite in eastern Spitsbergen (Senger et al., 2013;
478 Dallmann, 2015). In places, these sills are associated with areas showing high-frequency
479 disruptions of underlying sub-horizontal seismic reflections (dotted black lines in Figure 3f)
480 correlated with onshore occurrences of Pennsylvanian–Mesozoic sedimentary strata (Andresen et
481 al., 1992; Haremo and Andresen, 1992; Dallmann, 2015). We interpret these areas of high-
482 frequency disruption in otherwise relatively undisturbed and only mildly deformed Pennsylvanian–
483 Mesozoic sedimentary strata as zones with occurrences of Cretaceous feeder dykes. Alternatively,
484 disruption may be related to scattering and attenuation of seismic energy caused on the sills.

485

486 *Stappen High (northwestern Norwegian Barents Sea north of Bjørnøya)*

487 On the Stappen High between Bjørnøya and Spitsbergen (Figure 1c), seismic reflections at
488 depth of 2–6 seconds (TWT) are dominated by moderate- to high-amplitude reflections with
489 limited (< 5 kilometers) lateral continuity showing asymmetric, dominantly SSW-leaning
490 curving geometries with a few hundreds of meters to a few kilometers width (yellow lines within
491 pink unit in Figure 3c), i.e., analogous to those in folded Precambrian basement rocks farther north
492 (Figure 3a and Figure 4a). These reflections are truncated by gently to moderately NNE- (and
493 subsidiary SSW-) dipping disruption surfaces (black lines within pink and purple units in Figure
494 3c), some of which connect upwards with shallow (0–2 seconds TWT), NNE-dipping, high-angle



495 listric disruptions near Bjørnøya in the south (red lines in Figure 3c). Notably, major seismic
496 reflections near the upwards termination of deep, moderately–gently NNE-dipping disruption
497 surfaces display characteristic gently curving-upwards geometries (yellow lines within pink and
498 purple units in Figure 3c) and overlying seismic onlaps (white half arrows in Figure 3c) similar to
499 those observed just south of major NNE-dipping thrust systems in Storfjorden and the northeastern
500 Norwegian Barents Sea (Figure 3a and supplement S2).

501 We interpret deep (2–6 seconds TWT), curving, discontinuous seismic reflections ((yellow
502 lines within pink and purple units in Figure 3c) as folded Precambrian–lower Paleozoic basement
503 rocks, and dominantly NNE-dipping disruption surfaces (black lines within pink and purple units
504 in Figure 3) as brittle–ductile thrust possibly partly mylonitic, though with less intense deformation
505 than the major NNE-dipping thrust systems observed farther north in Storfjorden and the
506 northeastern Norwegian Barents Sea, like the Kongsfjorden–Cowanodden fault zone. These
507 brittle–ductile thrusts can be traced eastwards on seismic data on the Stappen High and into the
508 Sørkapp Basin (Figure 1c).

509 Based on their geometries and on gentle folding of the seafloor reflection (yellow lines
510 within green unit in Figure 3c), shallow, NNE-dipping, high-angle listric disruptions are interpreted
511 as mildly inverted normal faults overprinting deep NNE-dipping thrusts. Based on previous
512 fieldwork on Bjørnøya (Worsley et al., 2001), on seismic mapping in the area (Lasabuda et al.,
513 2018), and on well tie to Hopen and Edgeøya, relatively continuous (> five kilometers) shallow
514 (0–2 seconds TWT), gently curved–undulating seismic reflections overlying folded Precambrian–
515 lower Paleozoic basement rocks are interpreted as mildly folded upper Paleozoic–Mesozoic (–
516 Cenozoic?) sedimentary strata (orange and green units in Figure 3c).

517

518 ***Potential field data and regional gravimetric and magnetic anomalies***

519 *NNE-dipping thrusts*

520 In the northern Barents Sea, Storfjorden and central–eastern Spitsbergen, the seismic
521 occurrences of the Kongsfjorden–Cowanodden, Bellsundbanken and Kinnhøgda–
522 Daudbjørnpynten fault zones coincide with gradual, step-like, southwards increases in gravimetry
523 and, in places, with high magnetic anomalies in cross-section (Figure 3a–b and d–f). Similar
524 southwards gradual and step-like increases in the Bouguer and magnetic anomalies correlate with
525 major thrusts north of Bjørnøya (Figure 3c; see Figure 1b for location of Bjørnøya). These patterns



526 suggest that the footwall of the thrust systems consists of relatively denser rock units, which is
527 supported by seismic interpretation showing thickening of metamorphosed and folded Precambrian
528 basement rock units (pink unit in Figure 3a and c–d) in the footwall of the thrusts.

529 In map-view gravimetric and magnetic data, the three thrust systems in Storfjorden (black
530 lines in Figure 3a) coincide with three high, WNW–ESE-trending, continuous, gently undulating
531 (and, in place, merging/splaying) gravimetric and discontinuous magnetic anomalies (dashed
532 yellow lines in Figure 5a–c) that are separated from each other by areas showing relatively low
533 gravimetric and magnetic anomalies (e.g., see green to blue areas in Figure 5a). Some of these
534 anomalies extend from central Spitsbergen to Storfjorden and the northern Barents Sea (below the
535 Ora and Olga basins) as curving, E–W- and NW–SE-trending, 50–100 kilometers wide anomalies
536 (dashed yellow lines in Figure 5a–c). Analogously, thrust systems north of Bjørnøya (Figure 3c)
537 and north of the Ora and Olga basins (supplement S2b) correlate with comparable WNW–ESE-
538 trending, curving magnetic and gravimetric anomalies (dashed yellow lines in Figure 5a–c). The
539 WNW–ESE-trending anomalies appear clearer by using a slope-direction shader, which
540 accentuates the contrast between each trend of anomalies (green and red areas in Figure 5b).

541 Most of the recognized, regional WNW–ESE-trending magnetic and gravimetric anomalies
542 (dashed yellow lines in Figure 5a–c) can be traced into the Russian Barents Sea where they are
543 linear and are crosscut by major N–S- to NNW–SSE-trending anomalies (dashed black and white
544 lines in Figure 5a–c). Subtle WNW–ESE-trending magnetic and gravimetric anomalies further
545 extend onshore northwestern Russia (e.g., Kanin Peninsula and southern Novaya Zemlya) where
546 they correlate with major Timanian thrusts and folds, some of which are suspected to extend
547 thousands of kilometers between northwestern Russia and the Varanger Peninsula in northern
548 Norway (e.g., Trollfjorden–Komagelva Fault Zone and Central Timan Fault; Siedlecka, 1975;
549 Siedlecka and Roberts, 1995; Olovyanishnikov et al., 2000; Kostyuchenko et al., 2006). In addition,
550 two of the southernmost WNW–ESE-trending gravimetric and magnetic anomalies coincide with
551 the location of well known, crustal-scale, SSW-verging Timanian thrust faults, the Trollfjorden–
552 Komagelva Fault Zone and the Central Timan Fault. Thus, based on their overall WNW–ESE
553 trend, patterns of alternating highs and lows both for gravimetric and magnetic anomalies (see
554 Figure 5a), location at the boundary of oppositely dipping slopes (see slope-direction shader map
555 in Figure 5b), and extensive field studies and seismic and well data in northwestern Russia (e.g.,
556 Kanin Peninsula and Timan Range; Siedlecka and Roberts, 1995; Olovyanishnikov et al., 2000;



557 Kostyuchenko et al., 2006) and northern Norway (e.g., Varanger Peninsula; Siedlecka, 1975),
558 WNW–ESE-trending anomalies are interpreted as a combination of basement-seated Timanian
559 macrofolds and top-SSW reverse faults (Figure 5a–c).

560

561 *N–S-trending folds*

562 Large N–S-trending open folds (e.g., black and yellow lines in Figure 3b) coincide with N–
563 S- to NNE–SSW-trending, 20–100 kilometers wide, arcuate gravimetric and magnetic anomalies
564 (dashed white and black lines in Figure 5a–c), which are highly oblique to WNW–ESE-trending
565 gravimetric and magnetic anomalies and thrust systems (dashed yellow lines in Figure 5a–c).
566 Notably, major N–S- to NNE–SSW-trending synclines in Figure 3b (marked as red lines over a
567 white line in Figure 5a and c and as pink lines over a red line in Figure 5b) coincides with similarly
568 trending gravimetric and magnetic anomalies (dashed black lines in Figure 5a and c and dashed
569 white lines in Figure 5b). On the slope-direction shader map, these N–S- to NNE–SSW-trending
570 anomalies are localized along the boundary between areas with eastwards- (ca. 90–100°; blue areas
571 in Figure 5b) and westwards-facing slopes (ca. 270–280°; white areas in Figure 5b).

572 Notably where the main thrusts are preserved, major N–S-trending synforms (see 50–60
573 kilometers wide U-shaped depression formed by the Kinnhøgda–Daudbjørnpynten fault zone, i.e.,
574 black lines, in Figure 3b) coincide with gravimetric and magnetic highs (white and black dashed
575 lines in Figure 5a–c), whereas major antiforms where major NNE-dipping thrusts are partly eroded
576 (e.g., c. 100 kilometers wide areas where the Kinnhøgda–Daudbjørnpynten fault zone is absent in
577 Figure 3b) coincide with gravimetric and magnetic lows (the lows are parallel to white and black
578 dashed lines symbolizing magnetic and gravimetric highs in Figure 5a–c). The correlation of the
579 interpreted NNE-dipping thrust systems with gravimetric highs suggests that the thrusts consist of
580 relatively denser rocks. This supports the inferred mylonitic component of the thrusts because
581 mylonites are relatively denser due to the formation of high-density minerals with increasing
582 deformation (e.g., Arbaret and Burg, 2003; Colomby et al., 2015).

583 In the northwestern part of the Barents Sea (i.e., area covered by seismic data presented in
584 Figure 3), N–S- to NNE–SSW-trending gravimetric and magnetic anomalies (white and black
585 dashed lines in Figure 5a–c) are typically 20–50 kilometers wide and correlate with similarly
586 trending Caledonian folds and thrusts onshore Nordaustlandet (e.g., Rijpdalen Anticline; Johansson
587 et al., 2004; 2005; Dumais and Brønner, 2020) and northeastern Spitsbergen (e.g., Atomfjella



588 Antiform; Gee et al., 1994; Witt-Nilsson et al., 1998), whose width is comparable to that of the
589 anomalies. In the south, N–S- to NNE–SSW-trending gravimetric and magnetic anomalies merge
590 together and swing into a NE–SW trend onshore–nearshore the Kola Peninsula and northern
591 Norway. These anomalies mimic the attitude of Caledonian thrusts and folds in the southern
592 Norwegian Barents Sea (Gernigon and Brönnert, 2012; Gernigon et al., 2014) and onshore northern
593 Norway (Sturt et al., 1978; Townsend, 1987; Roberts and Williams, 2013). In the east, N–S- to
594 NNE–SSW-trending anomalies broaden to up to 150 kilometers in the Russian Barents Sea (Figure
595 5a–c).

596 In places, the intersections of high, WNW–ESE- and N–S- to NNE–SSW-trending
597 gravimetric and magnetic anomalies generate relatively higher, oval-shaped anomalies (e.g., dotted
598 white lines in Figure 5a and c). Notable examples are found in the Ora and Olga basins and east
599 and south of these basins (see dotted white lines in Figure 5a and c).

600

601 **Discussion**

602 In the discussion, we consider the lateral extent of the interpreted NNE-dipping thrust
603 systems, their possible timing of formation, and potential episodes of reactivation and overprinting.
604 Then we briefly discuss the implications of these thrust systems for plate tectonics reconstructions
605 in the Arctic.

606

607 *Extent of NNE-dipping thrust systems*

608 Four major NNE-dipping systems of mylonitic thrusts and shear zones (Steiløya–Krylen,
609 Kongsfjorden–Cowanodden, Bellsundbanken, Kinnhøgda–Daudbjørnpynten fault zones) were
610 identified at depths > 1–2 seconds (TWT) in central–eastern Spitsbergen, Storfjorden and the
611 northeastern Barents Sea, and several systems with less developed ductile fabrics between
612 Spitsbergen and Bjørnøya on the Stappen High (Figure 3a–f).

613 The Kongsfjorden–Cowanodden fault zone is relatively easy to trace and correlate in
614 Sassenfjorden, Sassendalen, Nordmannsfonna, Storfjorden and the northeastern Barents Sea (east
615 of Edgeøya) because (i) the seismic data in the these areas have a high resolution and good
616 coverage, (ii) internal seismic reflections are characterized by high amplitudes (e.g., brittle–ductile
617 thrusts and mylonitic shear zones), (iii) kinematic indicators within the thrust system consistently
618 show dominantly top–SSW sense of shear with SSW-verging fold structures (Figure 3a and d–f,



619 and supplement S2), (iv) the geometry and kinematics indicators along shallow brittle overprints
620 are regionally consistent (listric, down-NNE, brittle normal faults; Figure 3a and d–f), and (v) this
621 thrust consistently coincides with increase in gravimetric and magnetic anomaly in cross-section
622 (Figure 3a and d) and with analogously trending gravimetric and magnetic anomalies in central–
623 eastern Spitsbergen and the northern Barents Sea (Figure 5a–b). This thrust system was previously
624 identified below the Ora Basin by Klitzke et al. (2019), though interpreted as potential Timanian
625 grain instead of a discrete structure. The proposed correlation based on seismic, and cross-section
626 and map-view gravimetric and magnetic data suggests a lateral extent of c. 550–600 kilometers
627 along strike for the Kongsfjorden–Cowanodden fault zone. However, the regional magnetic and
628 gravimetric anomalies associated with this thrust in the Norwegian Barents Sea and Svalbard
629 extend potentially farther east as a series of WNW–ESE-trending anomalies to the mainland of
630 Russia (Figure 5a–c). Notably, these anomalies correlate with the southern edge of Novaya Zemlya
631 (Figure 5a–c) and, more specifically, with WNW–ESE-striking fault segments of the Baidaratsky
632 fault zone (Figure 1a; Lopatin et al., 2001; Korago et al., 2004), a major thrust fault that bounds a
633 major basement high in the central Russian Barents Sea, the Ludlov Saddle (Johansen et al., 1992;
634 Drachev et al., 2010). Thus, it is possible that the Kongsfjorden–Cowanodden fault zone also
635 extends farther east, possibly merging with the Baidaratsky fault zone, i.e., with a minimum extent
636 of 1700–1800 kilometers (Figure 5a–c).

637 The overall NNE-dipping and folded (into NNE-plunging folds) geometry of the
638 Kongsfjorden–Cowanodden fault zone (Figure 3e–f and Klitzke et al., 2019, their figures 3–5) may
639 explain the alternating NW–SE- and E–W-trending geometry of the gravimetric and magnetic
640 anomalies correlating with this thrust system (Figure 5a–b). E–W- and NW–SE-trending segments
641 of these anomalies may represent respectively the western and eastern limbs of open, gently NNE-
642 plunging macro-anticlines in the northern Norwegian Barents Sea. This is supported by the
643 relatively higher, oval-shaped gravimetric and magnetic anomalies at the intersection of WNW–
644 ESE- and N–S- to NNE–SSW-trending magnetic and gravimetric highs, which are interpreted as
645 the interaction of two sub-orthogonal fold trends (Figure 5a and c).

646 Interpretation of seismic sections (Figure 3e–f and supplement S2) and regional magnetic
647 and gravimetric data (Figure 5a–c) in central–eastern Spitsbergen show that NNE-dipping, top-
648 SSW Kongsfjorden–Cowanodden and Bellsundbanken fault zones likely extend westwards into
649 central (and possibly northwestern) Spitsbergen (e.g., Sassendalen, Sassenfjorden, Tempelfjorden,



650 and Billefjorden; see Figure 1c for locations). This is further supported by recent field, bathymetric
651 and seismic mapping in central Spitsbergen showing that (inverted) Devonian–Carboniferous
652 NNE-dipping brittle normal faults in Billefjorden and Sassenfjorden–Tempelfjorden merge with
653 kilometer-scale, NNE-dipping, Precambrian basement fabrics and shear zones at depth (Koehl,
654 2020a; Koehl et al., 2021 in review). Other examples of WNW–ESE-trending fabrics include faults
655 within Precambrian basement and Carboniferous sedimentary rocks in northeastern Spitsbergen
656 (Witt-Nilsson et al., 1998; Koehl and Muñoz-Barrera, 2018), and within Devonian sedimentary
657 rocks in northern and northwestern Spitsbergen (Friend et al., 1997; McCann, 2000; Dallmann and
658 Piepjohn, 2020). These suggest a repeated and regional influence of WNW–ESE-trending thrust
659 systems and associated basement fabrics in Spitsbergen.

660 Analogously to the Kongsfjorden–Cowanodden fault zone, the Bellsundbanken and
661 Kinnhøgda–Daudbjørnpynten fault zones (Figure 3a) geometries and kinematics on seismic data,
662 and their coinciding with parallel gravimetric and magnetic anomalies in map view and with
663 magnetic and gravimetric highs in cross-section suggest that they extend from Storfjorden to the
664 island of Hopen (Figure 1c, Figure 3a, Figure 5a–c, and supplement S2). Notably, a 50–100
665 kilometers wide, NNE–SSW-trending gravimetric and associated magnetic anomaly interpreted as
666 Caledonian grain in Nordaustlandet (Rijpdalen Anticline; Dumais and Brönnner, 2020) bends across
667 the trace of these two thrust systems (Figure 5a–c). Farther east, the Bellsundbanken and
668 Kinnhøgda–Daudbjørnpynten fault zones parallel gravimetric and magnetic, alternating E–W- and
669 NW–SE-trending anomalies that follow the trends and map-view shapes of the Ora and Olga basins
670 in the northeastern Norwegian Barents Sea (Anell et al., 2016; see Figure 1b–c for location). This
671 suggests that these two thrust systems extend into the northeastern Norwegian Barents Sea and,
672 potentially, into the Russian Barents Sea, and affected the development of Paleozoic sedimentary
673 basins. This is also the case of the Steiløya–Krylen fault zone (supplement S2b), which coincides
674 with mild, discontinuous, WNW–ESE-trending gravimetric and magnetic anomalies that extend
675 well into the Russian Barents Sea and, possibly, across Novaya Zemlya (Figure 5a–c).

676 In southwestern Spitsbergen, field mapping revealed the presence of a major, subvertical,
677 kilometer-thick, WNW–ESE-striking mylonitic shear zone metamorphosed under amphibolite
678 facies conditions, the Vimsodden–Kosibapasset Shear Zone (Majka et al., 2008, 2012; Mazur et
679 al., 2009; see Figure 1c for location). This major sinistral shear zone aligns along a WNW–ESE-
680 trending axis with the Kinnhøgda–Daudbjørnpynten fault zone in the northwestern Norwegian



681 Barents Sea (Figure 3a), and shows a folded geometry in map view that is comparable to that of
682 major NNE-dipping thrust systems in the northern Norwegian Barents Sea (Figure 3a and e–f,
683 Figure 5a–c, and supplement S2; Klitzke et al., 2019). In addition, the Vimsodden–Kosibapasset
684 Shear Zone juxtaposes relatively old Proterozoic basement rocks in the north against relatively
685 young rocks in the south, thus suggesting a similar configuration and kinematics as along the
686 Kinnhøgda–Daudbjørnpynten fault zone in Storfjorden and the northeastern Norwegian Barents
687 Sea. Moreover, von Gosen and Piepjohn (2001) and Bergh and Grogan (2003) reported that
688 Devonian–Mississippian sedimentary successions and Cenozoic fold structures (e.g., Hyrnefjellet
689 Anticline) are offset sinistrally by a few kilometers in Hornsund. Thus, we propose that the
690 Vimsodden–Kosibapasset Shear Zone extends into Hornsund and represents the westwards
691 continuation of the Kinnhøgda–Daudbjørnpynten fault zone. This suggests a minimum extent of
692 400–450 kilometers for this thrust system (Figure 1b–c and Figure 5a–c).

693

694 ***Timing of formation of major NNE-dipping thrust systems and N–S-trending folds***

695 *NNE-dipping thrust systems*

696 The several-kilometer thickness and hundreds–thousands of kilometers along-strike extent
697 of NNE-dipping thrust systems in central–eastern Spitsbergen, Storfjorden, and the northwestern
698 and northeastern Norwegian Barents Sea suggest that they formed during a major contractional
699 tectonic event. The overall WNW–ESE trend and the consistent north-northeastwards dip and top-
700 SSW sense of shear along the newly evidenced deep thrust systems preclude formation during the
701 Grenvillian, Caledonian, and Ellesmerian orogenies, and the Eureka tectonic event. These tectonic
702 events all involved dominantly E–W-oriented contraction and resulted in the formation of overall
703 N–S- to NNE–SSW-trending fabrics, structures and deformation belts in Svalbard (i.e., sub-
704 orthogonal to the newly identified thrust systems) such as the Atomfjella Antiform (Gee et al.,
705 1994; Witt-Nilsson et al., 1998), the Vestfonna and Rijpdalen anticlines (Johansson et al., 2004;
706 2005; Dumais and Brønner, 2020), the Dickson Land and Germaniahelvøya fold-thrust zones
707 (McCann, 2000; Piepjohn, 2000; Dallmann and Piepjohn, 2020), and the West Spitsbergen Fold-
708 and-Thrust Belt and related early Cenozoic structures in eastern Spitsbergen (Andresen et al., 1992;
709 Haremo and Andresen, 1992; Dallmann et al., 1993), and NE–SW- to NNE–SSW-striking thrusts
710 and folds in northern Norway (Sturt et al., 1978; Townsend, 1987; Roberts and Williams, 2013)
711 and the southwestern Barents Sea (Gernigon et al., 2014).



712 A possible cause for the formation of the observed NNE-dipping thrust systems is the late
713 Neoproterozoic Timanian Orogeny, which is well known onshore northwestern Russia (e.g., Kanin
714 Peninsula, Timan Range and central Timan; Siedlecka and Roberts, 1995; Olovyanishnikov et al.,
715 2000; Kostyuchenko et al., 2006) and northeastern Norway (Varanger Peninsula; Siedlecka and
716 Siedlecki, 1967; Siedlecka, 1975; Roberts and Olovyanishnikov, 2004), and traces of which were
717 recently found in southwestern Spitsbergen (Majka et al., 2008, 2012, 2014) and northern
718 Greenland (Rosa et al., 2016; Estrada et al., 2018). The overall transport direction during this
719 orogeny was directed towards the south-southwest and most thrust systems show NNE-dipping
720 geometries (Olovyanishnikov et al., 2000; Kostyuchenko et al., 2006), e.g., the Timanian thrust
721 front on the Varanger Peninsula in northeastern Norway (Trollfjorden–Komagelva Fault Zone;
722 Siedlecka and Siedlecki, 1967; Siedlecka, 1975). In addition, the size of Timanian thrust systems
723 in the Timan Range (e.g., Central Timan Fault) is comparable ($\geq 3\text{--}4$ seconds TWT; Kostyuchenko
724 et al., 2006 their figure 17) to that of thrust systems in the northern Norwegian Barents Sea and
725 Svalbard (Figure 3a and c–d).

726 Thus, based on their overall WNW–ESE strike (Figure 1b–c), their vergence to the south-
727 southwest (Figure 3a, c–d and f), their coincidence with gravimetric and magnetic highs (Figure
728 5a–c), their upward truncation by a major unconformity consistently throughout the study area (see
729 top-Precambrian unconformity in Figure 3a–d), and the correlation of these NNE-dipping thrusts
730 (via gravimetric and magnetic anomalies) to similarly striking and verging structures of comparable
731 size (i.e., several seconds TWT thick) onshore–nearshore northwestern Russia and northern
732 Norway (Siedlecka, 1975; Siedlecka and Roberts, 1995; Olovyanishnikov et al., 2000; Roberts and
733 Siedlecka, 2002; Gee and Pease, 2004; Kostyuchenko et al., 2006), NNE-dipping thrusts in the
734 northern Norwegian Barents Sea, Storfjorden, and central–eastern Spitsbergen are interpreted as
735 the western continuation of Timanian thrusts.

736 Timanian grain was recently identified in the northeastern Norwegian Barents Sea through
737 interpretation of new seismic, magnetic and gravimetric datasets shown in Figure 5a–c (Klitzke et
738 al., 2019). The alignment, coincident location, and matching geometries (e.g., curving E–W to
739 NW–SE strike/trend and kilometer-wide NNE–SSW-trending anticline) between Timanian grain
740 and structures mapped by Klitzke et al. (2019) and the major, NNE-dipping, top-SSW thrust
741 systems described in central–eastern Spitsbergen, Storfjorden and the Norwegian Barents Sea
742 (Figure 3a–f and supplement S2) further support a Timanian origin for the latter. Further evidence



743 of relic Timanian structural grain as far as the Loppa High and Bjørnøya Basin are documented by
744 previous magnetic studies and modelling (Marello et al., 2010). Moreover, seismic mapping
745 suggests that Timanian thrust systems extend well into central Spitsbergen (Figure 3e–f and
746 supplement S2c–d; Koehl, 2020a; Koehl et al., 2021 in review), and regional gravimetric and
747 magnetic anomaly maps suggest that Timanian thrust systems might extend farther west to (north-
748) western Spitsbergen (Figure 5a–c).

749 Probable reasons as to why these major (hundreds–thousands of kilometers long) thrust
750 systems were not identified before during fieldwork in Svalbard are their burial to high depth (>
751 1–2 seconds TWT in the study area, i.e., several kilometers below the surface; Figure 3a–f), and
752 their strong overprinting by younger tectonic events like the Caledonian Orogeny in areas where
753 they are exposed (e.g., Vimsodden–Kosibapasset Shear Zone in southwestern Spitsbergen;
754 Faehnrich et al., 2020). Possible areas of interest for future studies include the western and
755 northwestern parts of Spitsbergen where Caledonian and Eureka E–W contraction contributed to
756 uplift and exhume deep basement rocks, and where Timanian rocks potentially crop out (e.g.,
757 Peucat et al., 1989).

758

759 *N–S-trending folds*

760 N–S-trending upright folds involve the NNE-dipping thrust systems (Figure 3b and e) and
761 correlate (via gravimetric and magnetic anomalies) with major Caledonian folds in northeastern
762 Spitsbergen and Nordaustlandet, like the Atomfjella Antiform (Gee et al., 1994; Witt-Nilsson et
763 al., 1998) and Rjipdalen Anticline (Johansson et al., 2004; 2005; Dumais and Brønner, 2020), with
764 Caledonian grain in the southern Norwegian Barents Sea (Gernigon and Brønner, 2012; Gernigon
765 et al., 2014), and with major NE–SW-trending Caledonian folds onshore northern Norway (Sturt
766 et al., 1978; Townsend, 1987; Roberts and Williams, 2013). In addition, the width of the NE–SW-
767 to N–S-trending gravimetric and magnetic anomalies associated with these folds increases up to
768 150 kilometers eastwards, i.e., away from the Caledonian collision zone (Figure 5a–c; Corfu et al.,
769 2014; Gasser, 2014). Thus, N–S-trending folds in the northern Norwegian Barents Sea are
770 interpreted as Caledonian regional folds in Precambrian–lower Paleozoic rocks. The relatively
771 broader geometry of Caledonian folds away from the Caledonian collision zone (e.g., in the
772 Russian Barents Sea) is inferred to be related to gentler fold geometries due to decreasing
773 deformation intensity in this direction. This is further supported by relatively low grade Caledonian



774 metamorphism in Franz Josef Land (Knudsen et al., 2019; see Figure 1a–b for location). By
775 contrast, the presence of tighter Caledonian folds near the collision zone in the northern Norwegian
776 Barents Sea (e.g., Figure 3b and e, and Atomfjella Antiform and Rijpdalen Anticline onshore; Gee
777 et al., 1994; Witt-Nilsson et al., 1998; Johansson et al., 2004, 2005; Dumais and Brönnér, 2020) is
778 associated with much narrower (20–50 kilometers wide) gravimetric and magnetic anomalies
779 (Figure 5a–c). Note that the Atomfjella Antiform and Rijpdalen Anticline can be directly correlated
780 with 20–50 kilometers wide, N–S-trending high gravimetric and magnetic anomalies (Figure 5a–
781 c). Noteworthy, some of the NNE–SSW-trending folds and anomalies in the northernmost
782 Norwegian Barents Sea may reflect a combination of Caledonian and superimposed early Cenozoic
783 Eureka folding (e.g., Kairanov et al., 2018).

784 The interference of WNW–ESE- and N–S- to NNE–SSW-trending gravimetric highs,
785 which are correlated to Timanian and Caledonian folds respectively, produces oval-shaped
786 gravimetric and magnetic highs (Figure 5a). These relatively higher, oval-shaped gravimetric
787 anomalies are interpreted to correspond to dome-shaped folds resulting from the interaction of
788 Timanian and Caledonian folds involving refolding of WNW–ESE-trending Timanian folds during
789 E–W Caledonian contraction. This interpretation is supported by field studies on the Varanger
790 Peninsula in northern Norway and by seismic studies of Timanian thrusts off northern Norway
791 where the interaction of Timanian and Caledonian folds produced dome-shaped fold structures
792 (Ramsay, 1962), e.g., like the Ragnarokk Anticline (Siedlecka and Siedlecki, 1971; Koehl, in
793 prep.). Furthermore, Barrère et al. (2011) suggested that basins and faults in the southern
794 Norwegian Barents Sea are controlled by the interaction of Caledonian and Timanian structural
795 grain, and Marello et al. (2010) argued that elbow-shaped magnetic anomalies reflect the
796 interaction of Caledonian and Timanian structural grains in the Barents Sea, potentially as far west
797 as the Loppa High and the Bjørnøya Basin.

798

799 ***Phanerozoic reactivation and overprinting of Timanian thrust systems***

800 *Caledonian reactivation and overprint*

801 The geometry of the Kongsfjorden–Cowanodden and Kinnhøgda–Daudbjørnpynten fault
802 zones in Nordmannsfonna (Figure 3e) and the northeastern Norwegian Barents Sea (Figure 3b;
803 Klitzke et al., 2019), where they are folded into broad NNE-plunging upright anticlines and
804 synclines suggests that these thrust systems were deformed after they accommodated top-SSW



805 Timanian thrusting (Figure 6a and Figure 7a). In addition, subsidiary top-west kinematics (west-
806 verging folds and top-west minor thrusts) suggest that these thrust systems were partly reactivated–
807 overprinted during an episode of intense E–W contraction (Figure 6b and Figure 7b). However,
808 west-dipping dykes crosscutting and gently east-dipping sedimentary strata overlying the eastern
809 part of the folded Kongsfjorden–Cowanodden fault zone are only mildly folded, and upper
810 Paleozoic sedimentary strata lie flat over folded and partly eroded Precambrian–lower Paleozoic
811 rocks and the Kinnhøgda–Daudbjørnpynten fault zone, thus suggesting that these sedimentary
812 strata and dykes were not involved in this episode of E–W contraction (Figure 3e).

813 A notable episode of E–W contraction in Svalbard is the Caledonian Orogeny in the early–
814 mid Paleozoic, which resulted in the formation of west-verging thrusts and N–S-trending folds of
815 comparable size (c. 15–25 kilometers wide) to those affecting the Kongsfjorden–Cowanodden and
816 Kinnhøgda–Daudbjørnpynten fault zones in Nordmannsfonna and the northern Norwegian Barents
817 Sea (Figure 3b and e; Klitzke et al., 2019, their figures 3–5), such as the Atomfjella Antiform in
818 northeastern Spitsbergen (Gee et al., 1994; Witt-Nilsson et al., 1998; Lyberis and Manby, 1999)
819 and the Rijpdalen Anticline in Nordaustlandet (Figure 1b). Since the NNE-plunging anticline in
820 Nordmannsfonna does not affect overlying Pennsylvanian–Mesozoic sedimentary strata (Figure
821 3e), we propose that they formed during Caledonian contraction (Figure 7b). This is supported by
822 the involvement of the top-Precambrian unconformity and underlying NNE-dipping thrusts in N–
823 S- to NNE-SSW-trending folds, and by the truncation of these folds by the top-Silurian
824 unconformity, which is overlapped by mildly deformed to flat-lying upper Paleozoic strata (Figure
825 3b and Figure 4f). Furthermore, structures with geometries comparable to NNE-plunging folds in
826 the northern Barents Sea and Svalbard were observed in northern Norway. An example is the
827 Ragnarokk Anticline, a dome-shaped fold structure along the Timanian front thrust on the Varanger
828 Peninsula, which results from the re-folding of Timanian thrusts and folds into a NE–SW-trending
829 Caledonian trend (Siedlecka and Siedlecki, 1971).

830 Further support of a Caledonian origin for upright NNE-plunging folds in eastern
831 Spitsbergen, Storfjorden and the northern Norwegian Barents Sea is that these folds are relatively
832 tight in the west, in Nordmannsfonna and the northwestern Barents Sea (Figure 3b and e), whereas
833 they show gradually gentler and more open geometries in the east, i.e., away from the Caledonian
834 collision zone (Figure 3b). This is also shown by the gradual eastwards broadening of regional
835 gravimetric and magnetic anomalies correlated with Caledonian folds suggesting gentler fold



836 geometries related to decreasing (Caledonian) deformation intensity in this direction (Figure 5a–
837 c). This contrasts with the homogeneous intensity of deformation along NNE-dipping thrusts on
838 seismic data and with the homogeneous width of related gravimetric–magnetic anomalies from
839 west to east in Svalbard and the Barents Sea (Figure 3a–f and Figure 5a–c and supplement S2).

840 In Nordmannsfonna, the Caledonian origin of the major 15–20 kilometers wide anticline,
841 and the truncation of overlying, gently east-dipping, mildly folded sedimentary strata and
842 crosscutting west-dipping dykes by the base-Pennsylvanian unconformity suggest that these
843 sedimentary strata and dykes are Devonian (–Mississippian?) in age (Figure 6c–d). This is
844 supported by the presence of thick Devonian–Mississippian collapse deposits in adjacent areas of
845 central–northern Spitsbergen (Cutbill et al., 1976; Murascov and Mokin, 1979; Aakvik, 1981;
846 Gjelberg, 1983; Manby and Lyberis, 1992; Friend et al., 1997), and by Middle Devonian to
847 Mississippian ages (395–327 Ma) for dykes in central–northern Spitsbergen (Evdokimov et al.,
848 2006), northern Norway (Lippard and Prestvik, 1997; Guise and Roberts, 2002), and northwestern
849 Russia (Roberts and Onstott, 1995).

850 The occurrence of a > 0.5 second (TWT) reverse offset of the folded Kongsfjorden–
851 Cowanodden fault zone and the lack of offset of the Devonian (–Mississippian?) dykes across the
852 Agardhbukta Fault indicate that the latter fault formed as a top-west thrust during the Caledonian
853 Orogeny. At depth, the Agardhbukta Fault merges with the eastern flank of the folded
854 Kongsfjorden–Cowanodden fault zone. This, together with the presence of minor, high-angle, top-
855 west brittle thrusts within the Kongsfjorden–Cowanodden fault zone (Figure 3e), indicates that the
856 Agardhbukta Fault reactivated and/or overprinted the eastern portion of the Kongsfjorden–
857 Cowanodden fault zone in Nordmannsfonna during Caledonian contraction (Figure 6b and Figure
858 7b). Depth conversion using seismic velocities from Gernigon et al. (2018) suggest that the
859 Agardhbukta Fault offset the Kongsfjorden–Cowanodden fault zone by ca. 2.4–2.5 kilometers top-
860 west during Caledonian contraction (Figure 3e and supplement S3g). These kinematics are
861 consistent with field observation in eastern Spitsbergen by Piepjohn et al. (2019, their figure 17b).
862 However, Piepjohn et al. (2019) also suggested a significant component of Mesozoic–Cenozoic,
863 down-east normal movement, which was not identified in Nordmannsfonna. This suggests either
864 along strike variation in the movement history of the Agardhbukta Fault, either that the fault
865 mapped on seismic data in Nordmannsfonna does not correspond to the Agardhbukta Fault of
866 Piepjohn et al. (2019).



867 Considering the presence of crustal-scale, NNE-dipping, hundreds (to thousands?) of
868 kilometers long (Timanian) thrust systems extending from the Barents Sea (and possibly from
869 onshore Russia) to central–eastern and southern Spitsbergen and the northwestern Norwegian
870 Barents Sea (Figure 5a–c) prior to the onset of E–W-oriented Caledonian contraction, it is probable
871 that such large structures would have (at least partially) been reactivated and/or overprinted during
872 subsequent tectonic events if suitably oriented. Under E–W contraction, WNW–ESE-striking,
873 dominantly NNE-dipping Timanian faults would be oriented at c. 30° to the direction of principal
874 stress and, therefore, be suitable (according to Anderson’s stress model) to reactivate/be
875 overprinted with sinistral strike-slip movements. Such kinematics were recorded along the
876 Vimsodden–Kosibapasset Shear Zone in Wedel Jarlsberg Land (Mazur et al., 2009) and within
877 Hornsund (von Gosen and Piepjohn, 2001).

878 However, recent ^{40}Ar – ^{39}Ar geochronological determinations on muscovite within this
879 structure suggest that this structure formed during the Caledonian Orogeny (Faehnrich et al. 2020).
880 Nonetheless, the same authors also obtained Timanian ages (600–540 Ma) for (initial) movements
881 along minor shear zones nearby and parallel to the Vimsodden–Kosibapasset Shear Zone. Since
882 this large shear zone must have represented a major preexisting zone of weakness when Caledonian
883 contraction initiated, it is highly probable that it was preferentially chosen to reactivate instead of
884 minor shear zones. Thus, the Caledonian ages obtained along the Vimsodden–Kosibapasset Shear
885 Zone most likely reflect complete resetting of the geochronometer along the shear zone due to large
886 amounts of Caledonian reactivation–overprinting, while minor nearby shear zones preserved traces
887 of initial Timanian deformation. This is also supported by observations in northern Norway
888 suggesting that Timanian thrusts (e.g., Trollfjorden–Komagelva Fault Zone) were reactivated as
889 major strike-slip faults during the Caledonian Orogeny (Roberts, 1972; Herrevold et al., 2009; Rice
890 2014). This interpretation reconciles the strong differences in dipping angle and depth between the
891 Kinnhøgda–Daudbjørnpynten fault zone and the Vimsodden–Kosibapasset Shear Zone. The
892 former was located away from the Caledonian collision zone and essentially retained its initial,
893 moderately NNE-dipping Timanian geometry and was deeply buried during the Phanerozoic,
894 whereas the latter was intensely deformed, pushed into a sub-vertical position, and uplifted an
895 exhumed to the surface because it was located near or within the Caledonian collision zone.

896

897 *Devonian–Carboniferous normal overprint–reactivation*



898 In Nordmannsfonna, the wedge shape of Devonian (–Mississippian?) sedimentary strata in
899 the hanging wall of the Kongsfjorden–Cowanodden fault zone suggest that the eastern portion of
900 this thrust was reactivated as a gently–moderately dipping extensional detachment (Figure 6c) and,
901 thus, that Devonian (–Mississippian?) strata in this area represent analogs to collapse deposits in
902 northern Spitsbergen. This is supported by the intrusion of west-dipping Devonian (–
903 Mississippian?) dykes orthogonal to the eastern portion of the thrust system, i.e., orthogonal to
904 extensional movements along the inverted east-dipping portion of the thrust (Figure 3e and Figure
905 6d). Similar relationships were inferred in northwestern Spitsbergen, where Devonian collapse
906 sediments were deposited along a N–S-trending Precambrian basement ridge bounded by a gently
907 dipping, extensional mylonitic detachment (Braathen et al., 2018).

908 In Sassenfjorden, Storfjorden and the northeastern Norwegian Barents Sea, listric brittle
909 normal faults showing down–NNE offsets and syn-tectonic thickening within Devonian–
910 Carboniferous (–Permian?) sedimentary strata merge at depth with the uppermost part of NNE-
911 dipping Timanian thrust systems like the Kongsfjorden–Cowanodden fault zone (Figure 3a and d
912 and supplement S2c). This indicates that Timanian thrust systems were used as preexisting zones
913 of weakness during late–post-orogenic collapse of the Caledonides in the Devonian–Carboniferous
914 (Figure 6c–e and Figure 7c).

915 The presence of the Kongsfjorden–Cowanodden fault zone in Storfjorden and below
916 Edgeøya also explains the strong differences between the Paleozoic sedimentary successions
917 penetrated by the Plurdalen-1 and Raddendalen-1 exploration wells (Bro and Shvarts, 1983;
918 Harland and Kelly, 1997). Notably, the Plurdalen-1 well penetrated (at least) ca. 1600 meters thick
919 Devonian–Mississippian sedimentary rocks in the direct hanging wall of the Kongsfjorden–
920 Cowanodden fault zone and related listric brittle overprints (Figure 3a), whereas the interpretation
921 of Bro and Shvarts (1983) suggests that the Raddendalen-1 well encountered thin (90–290 meters
922 thick) Mississippian strata overlying (> 2 kilometers) thick lower Paleozoic sedimentary rocks ca.
923 30 kilometers farther northeast, i.e., away from the Kongsfjorden–Cowanodden fault zone and
924 related overprints. The presence of thick Devonian sedimentary strata in the direct hanging wall of
925 listric overprints of the Kongsfjorden–Cowanodden fault zone further supports late–post-
926 Caledonian extensional reactivation–overprinting of NNE-dipping Timanian thrusts.

927 In central Spitsbergen, recently identified Early Devonian–Mississippian normal faults
928 formed along and overprinted–reactivated major NNE-dipping ductile (mylonitic) shear zones and



929 fabrics in Billefjorden (Koehl et al., 2021 in review) and Sassenfjorden–Tempelfjorden (Koehl,
930 2020a). These show sizes, geometries and kinematics comparable to those of the Kongsfjorden–
931 Cowanodden fault zone, and are, therefore, interpreted as the western continuation of this thrust
932 system. The Devonian–Carboniferous extensional reactivation–overprinting of the Kongsfjorden–
933 Cowanodden fault zone in central Spitsbergen explains the southward provenance of northwards
934 prograding sedimentary rocks of the uppermost Silurian–Lower Devonian Siktfejlet and Red Bay
935 groups and Wood Bay Formation and the enigmatic WNW–ESE trend of the southern boundary of
936 the Devonian Graben in central–northern Spitsbergen (Gee and Moody-Stuart, 1966; Friend et al.,
937 1966; Friend and Moody-Stuart, 1972; Murascov and Mokin, 1979; Friend et al., 1997; McCann,
938 2000; Dallmann and Piepjohn, 2020; Koehl et al., 2021 in review).

939

940 *Mild Triassic overprint*

941 The Kongsfjorden–Cowanodden fault zone and associated overprints align with WNW–
942 ESE- to NW–SE-striking normal faults onshore southern and southwestern Edgeøya in
943 Kvalpynten, Negerpynten, and Øhmanfjellet (Osmundsen et al., 2014; Ogata et al., 2018). These
944 faults display both listric and steep planar geometries in cross-section and bound thickened syn-
945 sedimentary growth strata in lowermost Upper Triassic sedimentary rocks of the Tschermakfjellet
946 and De Geerdalen formations (Ogata et al., 2018; Smyrak-Sikora et al., 2020). The Norwegian
947 Barents Sea and Svalbard are believed to have remained tectonically quiet throughout the Triassic
948 apart from minor deep-rooted normal faulting in the northwestern Norwegian Barents Sea (Anell
949 et al., 2013) and Uralides-related contraction in the (south-) east (Müller et al., 2019). Hence, we
950 propose that the progradation and accumulation of thick sedimentary deposits of the Triassic deltaic
951 systems above the southeastward continuation of the Kongsfjorden–Cowanodden fault zone may
952 have triggered minor tectonic adjustments resulting in the development of a system of small half-
953 grabens over the thrust system. Alternatively or complementary, the deposition of thick Triassic
954 deltaic systems may have locally accelerated compaction of sedimentary strata underlying the
955 Tschermakfjellet Formation in south- and southwest-Edgeøya, e.g., of the potential pre-Triassic
956 syn-tectonic growth strata along the Kongsfjorden–Cowanodden fault zone, and, thus, facilitated
957 the development of minor half-grabens within the Triassic succession along this thrust system.

958

959 *Eurekan reactivation–overprint*



960 In eastern Spitsbergen, the Agardhbukta Fault segment of the Lomfjorden Fault Zone
961 truncates the Kongsfjorden–Cowanodden fault zone with a major, > 0.5 second (TWT) top-west
962 reverse offset (Figure 3e). The Agardhbukta fault also mildly folds Pennsylvanian–Mesozoic
963 sedimentary rocks and Cretaceous sills into a gentle upright (fault-propagation) fold with no major
964 offset (Figure 6f–g), which is supported by onshore field observations in eastern and northeastern
965 Spitsbergen (Piepjohn et al., 2019). Mild folding of Mesozoic sedimentary rocks and of Cretaceous
966 intrusions indicates that the Agardhbukta Fault was most likely mildly reactivated as a top-west
967 thrust during the early Cenozoic Eurekan tectonic event (Figure 6g and Figure 7d).

968 Seismic data show that high-angle listric Devonian–Carboniferous normal faults were
969 mildly reactivated as reverse faults that propagated upwards and gently folded adjacent upper
970 Paleozoic–Mesozoic (–Cenozoic?) sedimentary strata in the northwestern Norwegian Barents Sea,
971 Storfjorden and central–eastern Spitsbergen (Figure 3a–c and supplement S2), but not in the
972 northeastern Norwegian Barents Sea (Figure 3d). Since normal faults were not inverted in the east,
973 it is probable that inversion of these faults in central–eastern Spitsbergen, Storfjorden and the
974 northwestern Norwegian Barents Sea first occurred during the Eurekan tectonic event in the early
975 Cenozoic, when Greenland collided with western Spitsbergen (Figure 7d). This is also supported
976 by the gently folded character of Devonian–Mesozoic (–Cenozoic?) sedimentary successions in
977 the west (Figure 3a and c), whereas these successions are essentially flat-lying (i.e., undeformed)
978 in the east (Figure 3b and d). Nevertheless, folding of the seafloor reflection in Storfjorden and the
979 northwestern Norwegian Barents Sea suggests ongoing contractional deformation along several of
980 these faults in the northwestern Norwegian Barents Sea and Storfjorden (Figure 3a–c).

981 Major, top-SSW mylonitic shear zones in Sassenfjorden–Tempelfjorden and Billefjorden
982 display early Cenozoic overprints including top-SSW duplexes in uppermost Devonian–
983 Mississippian coals of the Billefjorden Group acting as a partial décollement along a major
984 basement-seated listric brittle fault (Koehl, 2020a; supplement S2) and NNE-dipping brittle faults
985 offsetting the east-dipping Billefjorden Fault Zone by hundreds of meters to several kilometers left-
986 laterally (Koehl et al., 2021 in review). Thus, the correlation of the Kongsfjorden–Cowanodden
987 fault zone with these top-SSW mylonitic shear zones in Sassenfjorden–Tempelfjorden and
988 Billefjorden (see Figure 1c for location) supports reactivation–overprinting of major NNE-dipping
989 Timanian thrust systems as top-SSW, sinistral-reverse, oblique-slip thrusts in the early Cenozoic
990 Eurekan tectonic event. Such correlation explains the NW–SE trend and the location of the



991 northeastern boundary of the Central Tertiary Basin, which terminates just southwest of
992 Sassenfjorden and Sassendalen in central Spitsbergen (Figure 1b–c). It also explains the dominance
993 of NW–SE- to WNW–ESE-striking faults within Cenozoic deposits of the Central Tertiary Basin
994 (Livshits, 1965a), and the northwestwards provenance (Petersen et al., 2016) and northwards
995 thinning of sediments deposited in the basin (Livshits, 1965b), which were probably sourced from
996 uplifted areas in the hanging wall of the reactivated–overprinted thrust.

997 Noteworthy, Livshits (1965a) argued that the Central Tertiary Basin was bounded to the
998 north by a major WNW–ESE-striking fault extending from Kongsfjorden to southern Billefjorden–
999 Sassenjorden where the NNE-dipping Kongsfjorden–Cowanodden fault zone was mapped (present
1000 study; supplement S2). This indicates that the Kongsfjorden–Cowanodden fault zone might extend
1001 west of Billefjorden and Sassenfjorden, potentially until Kongsfjorden (see Figure 1c for location).
1002 Should it be the case, the Kongsfjorden–Cowanodden fault zone would coincide with a major
1003 terrane boundary in Svalbard, which was speculated to correspond to one or more regional WNW–
1004 ESE- to N–S-striking faults in earlier works, e.g., Kongsvegen Fault and Lapsdalen Thrust
1005 (Harland and Horsfield, 1974), Kongsvegen Fault Zone and/or Central–West Fault Zone (Harland
1006 and Wright, 1979), and Kongsfjorden–Hansbreen Fault Zone (Harland et al., 1993). The presence
1007 of a major, (inherited Timanian) NNE-dipping, basement-seated fault zone in this area would
1008 explain the observed strong differences between Precambrian basement rocks in Svalbard’s
1009 northwestern and southwestern terranes.

1010 In southern Spitsbergen, von Gosen and Piepjohn (2001) and Bergh and Grogan (2003)
1011 suggested the presence of a WNW–ESE-striking, sinistral-reverse strike-slip fault in Hornsund
1012 based on a one-kilometer left-lateral offset of Devonian–Carboniferous sedimentary successions
1013 and of the early Cenozoic Hyrnefjellet Anticline across the fjord. This fault is part of the
1014 Kinnhøgda–Daudbjørnpynten fault zone and was most likely reactivated–overprinted during
1015 Eurekan contraction–transpression in the early Cenozoic.

1016

1017 *Present day tectonism*

1018 Seismic data show that the seafloor reflection is folded and/or offset in a reverse fashion by
1019 high-angle brittle faults merging at depth with interpreted Timanian thrust systems in Storfjorden
1020 and just north of Bjørnøya in the northwestern Norwegian Barents (Figure 3a and c, and Figure
1021 4h). This indicates that some of the Timanian thrust systems are still active at present and are



1022 reactivated/overprinted by reverse faults (Figure 7e). A potential explanation for ongoing
1023 reactivation–overprinting is transfer of extensional tectonic stress in the Fram Strait as ridge-push
1024 tectonism through Spitsbergen and Storfjorden.

1025

1026 ***Implication for plate tectonics reconstructions of the Barents Sea and Svalbard in the late***
1027 ***Neoproterozoic–Paleozoic***

1028 The presence of hundreds to thousands of kilometers long Timanian faults throughout the
1029 northern Norwegian Barents Sea and central and southwestern (and possibly northwestern?)
1030 Spitsbergen indicates that the northwestern, northeastern and southwestern basement terranes of
1031 the Svalbard Archipelago were most likely already accreted together and attached to the Barents
1032 Sea, northern Norway and northwestern Russia in the late Neoproterozoic (ca. 600 Ma). Svalbard’s
1033 three terranes were previously thought to have been juxtaposed during the Caledonian and
1034 Ellesmerian orogenies through hundreds–thousands of kilometers of displacement along presumed
1035 thousands of kilometers long N–S-striking strike-slip faults like the Billefjorden Fault Zone
1036 (Harland, 1969; Harland et al. 1992, Labrousse et al., 2008; Figure 2). The presence of laterally
1037 continuous (undisrupted), hundreds–thousands of kilometers long, Timanian thrust systems from
1038 southwestern and central Spitsbergen to the northern Norwegian and Russian Barents Sea clearly
1039 shows that this is not possible.

1040 The continuous character of these thrust systems from potentially as far as onshore
1041 northwestern Russia through the Barents Sea and Svalbard precludes any major strike-slip
1042 displacement along N–S-striking faults such as the Billefjorden Fault Zone and Lomfjorden Fault
1043 Zone (as proposed by Harland et al., 1974, 1992; Labrousse et al., 2008) and any hard-linked
1044 connection between these faults in Svalbard and analogous, NE–SW-striking faults in Scotland in
1045 the Phanerozoic (as proposed by Harland, 1969). Instead, the present work suggests that the crust
1046 constituting the Barents Sea and the northeastern and southwestern basement terranes of Svalbard
1047 should be included as part of Baltica in future Arctic plate tectonics reconstructions for the late
1048 Neoproterozoic–Paleozoic period (i.e., until ca. 600 Ma). It also suggests that the Caledonian suture
1049 zone, previously inferred to lie east of Svalbard in the Barents Sea (e.g., Gee and Teben’kov, 2004;
1050 Breivik et al., 2005; Barrère et al., 2011; Knudsen et al., 2019) may be located west of the presently
1051 described Timanian thrust systems, i.e., probably west of or in western Spitsbergen where



1052 Caledonian blueschist and eclogite metamorphism was recorded in Precambrian basement rocks
1053 (Horsfield, 1972; Dallmeyer et al., 1990a; Ohta et al., 1995; Kosminska et al., 2014).

1054

1055 **Conclusions**

1056 1) Seismic data in the northern Norwegian Barents Sea and Svalbard reveal the existence of
1057 several systems of hundreds–thousands of kilometers long, several kilometers thick, top-
1058 SSW Timanian thrusts comprised of brittle–ductile thrusts, mylonitic shear zones and
1059 associated SSW-verging folds that appear to extend from onshore northwestern Russia to
1060 the northern Norwegian Barents Sea and to central and southwestern Spitsbergen. A notable
1061 structure is the Kongsfjorden–Cowanodden fault zone in Svalbard and the Norwegian
1062 Barents Sea, which likely merges with the Baidaratsky fault zone in the Russian Barents
1063 Sea and southern Novaya Zemlya.

1064 2) In the east (away from the Caledonian collision zone), these Timanian thrusts systems were
1065 folded into NNE-plunging folds, offset, and reactivated as and/or overprinted by top-west,
1066 oblique-slip sinistral-reverse, brittle–ductile thrusts during subsequent Caledonian (e.g.,
1067 Agardhbukta Fault segment of the Lomfjorden Fault Zone) and, possibly, during Eurekan
1068 contraction, and are deeply buried. By contrast, in the west (near or within the Caledonian
1069 collision zone), Timanian thrusts were intensely deformed, pushed into sub-vertical
1070 positions, extensively overprinted, and exhumed to the surface.

1071 3) In eastern Spitsbergen, a major NNE-dipping Timanian thrust system, the Kongsfjorden–
1072 Cowanodden fault zone, is crosscut by a swarm of Devonian (–Mississippian?) dykes that
1073 intruded contemporaneous sedimentary strata deposited during extensional reactivation of
1074 the eastern portion of the thrust system as a low-angle extensional detachment during late-
1075 post-Caledonian collapse.

1076 4) Timanian thrust systems were overprinted by NNE-dipping, brittle normal faults in the late
1077 Paleozoic during the collapse of the Caledonides and/or subsequent rifting in the Devonian–
1078 Carboniferous.

1079 5) Timanian thrust systems and associated Caledonian and Devonian–Carboniferous brittle
1080 overprints (e.g., Agardhbukta Fault) in the northwestern Norwegian Barents Sea and
1081 Svalbard were mildly reactivated during the early Cenozoic Eurekan tectonic event, which
1082 resulted in minor folding and minor reverse offsets of Devonian–Mesozoic sedimentary



1083 strata and intrusions. Timanian thrusts and related overprints in the northeastern Norwegian
1084 Barents Sea were not reactivated during the Eurekan tectonic event.

1085 6) The presence of hundreds–thousands of kilometers long Timanian thrust systems suggests
1086 that the Barents Sea and Svalbard’s three basement terranes were already attached to
1087 northern Norway and northwestern Russia in the late Neoproterozoic (ca. 600 Ma),
1088 precludes any major strike-slip movements along major N–S-striking faults like the
1089 Billefjorden and Lomfjorden fault zones in the Phanerozoic, and suggests that the
1090 Caledonian suture zone is located west of or in western Spitsbergen.

1091

1092 **Acknowledgements**

1093 The present study was supported by the Research Council of Norway, the Tromsø Research
1094 Foundation, and six industry partners through the Research Centre for Arctic Petroleum
1095 Exploration (ARCEX; grant number 228107), the SEAMSTRESS project (grant number 287865),
1096 and the Centre for Earth Evolution and Dynamics (CEED; grant number 223272). We thank the
1097 Norwegian Petroleum Directorate and the Federal Institute for Geosciences and Natural Resources
1098 (BGR) for granting access and allowing publication of seismic, magnetic and gravimetric data in
1099 Svalbard and the Norwegian Barents Sea. Prof. Steffen Bergh, Dr. Winfried Dallmann, Prof. Jiri
1100 Konopasek, Assoc. Prof. Mélanie Forien, Dr. Kate Waghorn (UiT The Arctic University of Norway
1101 in Tromsø), Dr. Peter Klitzke (Federal Institute for Geosciences and Natural Resources –
1102 Germany), Anna Dichiarante (Norway Seismic Array), Rune Matningsdal (Norwegian Petroleum
1103 Directorate), and Prof. Carmen Gaina (Centre for Earth Evolution and Dynamics, University of
1104 Oslo) are thanked for fruitful discussion.

1105

1106 **Data availability**

1107 For high-resolution versions of the figures and supplements, the reader is referred to the
1108 Open Access data repository DataverseNO (doi.org/10.18710/CE8RQH). The complete seismic
1109 study is also available from the corresponding author upon request.

1110

1111 **References**

1112 Aakvik, R.: Fasies analyse av Undre Karbonske kullførende sedimenter, Billefjorden, Spitsbergen,
1113 Ph.D. Thesis, University of Bergen, Bergen, Norway, 219 pp., 1981.



- 1114 Andresen, A., Haremo, P., Swensson, E. and Bergh, S. G.: Structural geology around the southern
1115 termination of the Lomfjorden Fault Complex, Agardhdalen, east Spitsbergen, Norsk Geol.
1116 Tidsskr., 72, 83–91, 1992.
- 1117 Anell, I., Braathen, A., Olaussen, S. and Osmundsen, P. T.: Evidence of faulting contradicts a
1118 quiescent northern Barents Shelf during the Triassic, *First Break*, 31, 67–76, 2013.
- 1119 Anell, I. M., Braathen, A. and Olaussen, S.: Regional constraints of the Sørkapp Basin: A
1120 Carboniferous relic or a Cretaceous depression, *Mar. Petrol. Geol.*, 54, 123–138, 2014.
- 1121 Anell, I. M., Faleide, J. I. and Braathen, A.: Regional tectono-sedimentary development of the
1122 highs and basins of the northwestern Barents Shelf, *Norsk Geologisk Tidsskrift*, 96, 1, 27–
1123 41, 2016.
- 1124 Arbaret, L. and Burg, J.-P.: Complex flow in lowest crustal, anastomosing mylonites: Strain
1125 gradients in a Kohistan gabbro, northern Pakistan, *J. Geophys. Res.*, 108, 2467, 2003.
- 1126 Barrère, C., Ebbing, J. and Gernigon, L.: Offshore prolongation of Caledonian structures and
1127 basement characterization in the western Barents Sea from geophysical modelling,
1128 *Tectonophys.*, 470, 71–88, 2009.
- 1129 Barrère, C., Ebbing, J. and Gernigon, L.: 3-D density and magnetic crustal characterization of the
1130 southwestern Barents Shelf: implications for the offshore prolongation of the Norwegian
1131 Caledonides, *Geophys. J. Int.*, 184, 1147–1166, 2011.
- 1132 Boyer, S. E. and Elliott, D.: Thrust Systems, *AAPG Bulletin*, 66, 9, 1196–1230, 1982.
- 1133 Braathen, A., Bælum, K., Maher Jr., H. D. and Buckley, S. J.: Growth of extensional faults and
1134 folds during deposition of an evaporite-dominated half-graben basin; the Carboniferous
1135 Billefjorden Trough, Svalbard, *Norsk Geol. Tidsskr.*, 91, 137–160, 2011.
- 1136 Braathen, A., Osmundsen, P. T., Maher, H. and Ganerød, M.: The Keisarhjelmen detachment
1137 records Silurian–Devonian extensional collapse in Northern Svalbard, *Terra Nova*, 30, 34–
1138 39, 2018.
- 1139 Breivik, A. J., Mjelde, R., Grogan, P., Shimamura, H., Murai, Y. and Nishimura, Y.: Caledonide
1140 development offshore–onshore Svalbard based on ocean bottom seismometer, conventional
1141 seismic, and potential field data, *Tectonophys.*, 401, 79–117, 2005.
- 1142 Bro, E. G. and Shvarts, V. H.: Processing results from drill hole Raddedalen-1, Edge Island,
1143 Spitzbergen Archipelago, All-Russian Research Institute for Geology and Mineral
1144 Resources of the World Ocean, St. Petersburg, Pangaea, Report 5750, 1983.



- 1145 Cawood, P. A., McCausland, P. J. A. and Dunning, G. R.: Opening Iapetus: Constraints from the
1146 Laurentian margin in Newfoundland, *GSA Bull.*, 113, 4, 443–453, 2001.
- 1147 Chalmers, J. A. and Pulvertaft, T. C. R.: Development of the continental margins of the Labrador
1148 Sea: a review, in: *Non-Volcanic Rifting of Continental Margins: A Comparison of*
1149 *Evidence from Land and Sea*, edited by: Wilson, R. C. L., Taylor, R. B. and Froitzheim,
1150 N., *Geol. Soc. London, Spec. Publi.*, 187, 77–105, 2001.
- 1151 Cocks, L. R. M. and Torsvik, T. H.: Baltica from the late Precambrian to mid-Palaeozoic times:
1152 The gain and loss of a terrane's identity, *Earth-Sci. Rev.*, 72, 39–66, 2005.
- 1153 Colomбу, S., Cruciani, G., Fancello, D., Franceschelli, M. and Musumeci, G.: Petrophysical
1154 properties of a granite-protomylonite-ultramylonite sequence: insight from the Monte
1155 Grighini shear zone, central Sardinia, Italy, *Eur. J. Mineral*, 27, 471–486, 2015.
- 1156 Corfu, F., Andersen, T. B. and Gasser, D.: The Scandinavian Caledonides: main features,
1157 conceptual advances and critical questions, in: *New Perspectives on the Caledonides of*
1158 *Scandinavia and Related Areas*, edited by: Corfu, F., Gasser, D. and Chew, D. M., *Geol.*
1159 *Soc., London, Spec. Publi.*, 390, 9–43, 2014.
- 1160 Cutbill, J. L. and Challinor, A.: Revision of the Stratigraphical Scheme for the Carboniferous and
1161 Permian of Spitsbergen and Bjørnøya, *Geol. Mag.*, 102, 418–439, 1965.
- 1162 Cutbill, J. L., Henderson, W. G. and Wright, N. J. R.: The Billefjorden Group (Early Carboniferous)
1163 of central Spitsbergen, *Norsk Polarinst. Skr.*, 164, 57–89, 1976.
- 1164 Dallmann, W. K.: *Geoscience Atlas of Svalbard*, Norsk Polarinstitut, Tromsø, Norway,
1165 Rapportserie nr. 148, 2015.
- 1166 Dallmann, W. K. and Krasil'scikov, A. A.: Geological map of Svalbard 1:50,000, sheet D20G
1167 Bjørnøya, *Norsk Polarinst. Temakart*, 27, 1996.
- 1168 Dallmann, W. K. and Piepjohn, K.: The structure of the Old Red Sandstone and the Svalbardian
1169 Orogenic Event (Ellesmerian Orogeny) in Svalbard, *Norg. Geol. Unders. B., Spec. Publi.*,
1170 15, 106 pp., 2020.
- 1171 Dallmeyer, R. D., Peucat, J. J., Hirajima, T. and Ohta, Y.: Tectonothermal chronology within a
1172 blueschist–eclogite complex, west-central Spitsbergen, Svalbard: Evidence from $^{40}\text{Ar}/^{39}\text{Ar}$
1173 and Rb–Sr mineral ages, *Lithos*, 24, 291–304, 1990a.



- 1174 Dallmeyer, R. D., Peucat, J. J. and Ohta, Y.: Tectonothermal evolution of contrasting metamorphic
1175 complexes in northwest Spitsbergen (Biskayerhalvøya): Evidence from $^{40}\text{Ar}/^{39}\text{Ar}$ and Rb-
1176 Sr mineral ages, *GSA Bull.*, 102, 653–663, 1990b.
- 1177 Dewey, J. F. and Strachan, R. A.: Changing Silurian–Devonian relative plate motion in the
1178 Caledonides: sinistral transpression to sinistral transtension, *J. Geol. Soc., London*, 160,
1179 219–229, 2003.
- 1180 Drachev, S. S.: Fold belts and sedimentary basins of the Eurasian Arctic, *Arktos*, 2:21, 2016.
- 1181 Drachev, S. S., Malyshev, N. A. and Nikishin, A. M.: Tectonic history and petroleum geology of
1182 the Russian Arctic Shelves: an overview, *Petrol. Geol. Conf. series*, 7, 591–619, 2010.
- 1183 Dumais, M.-A. and Brönnner, M.: Revisiting Austfonna, Svalbard, with potential field methods – a
1184 new characterization of the bed topography and its physical properties, *The Cryosphere*,
1185 14, 183–197, 2020.
- 1186 Eldholm, O. and Ewing, J.: Marine Geophysical Survey in the Southwestern Barents Sea, *J.*
1187 *Geophys. Res.*, 76, 17, 3832–3841, 1971.
- 1188 Engen, Ø., Faleide, J. I. and Dyreng, T. K.: Opening of the Fram Strait gateway: A review of plate
1189 tectonic constraints, *Tectonophys.*, 450, 51–69, 2008.
- 1190 Estrada, S., Tessensohn, F. and Sonntag, B.-L.: A Timanian island-arc fragment in North
1191 Greenland: The Midtkap igneous suite, *J. Geodyn.*, 118, 140–153, 2018.
- 1192 Faehnrich, K., Majka, J., Schneider, D., Mazur, S., Manecki, M., Ziemniak, G., Wala, V. T. and
1193 Strauss, J. V.: Geochronological constraints on Caledonian strike-slip displacement in
1194 Svalbard, with implications for the evolution of the Arctic, *Terra Nova*, 2020, 32, 290–299.
- 1195 Fortey, R. A. and Bruton, D. L.: Lower Ordovician trilobites of the Kirtonryggen Formation,
1196 Spitsbergen, *ossils and Strata*, 59, Wiley Blackwell, 120 pp., 2013.
- 1197 Fountain, D. M., Hurich, C. A. and Smithson, S. B.: Seismic relectivity of mylonite zones in the
1198 crust, *Geology*, 12, 195–198, 1984.
- 1199 Friend, P. F. and Moody-Stuart, M.: Sedimentation of the Wood Bay Formation (Devonian) of
1200 Spitsbergen: Regional analysis of a late orogenic basin, *Norsk Polarinst. Skr.*, 157, 80 pp.,
1201 1972.
- 1202 Friend, P. F., Heintz, N. and Moody-Stuart, M.: New unit terms for the Devonian of Spitsbergen
1203 and a new stratigraphical scheme for the Wood Bay Formation, *Polarinst. Årbok*, 1965, 59–
1204 64, 1966.



- 1205 Friend, P. F., Harland, W. B., Rogers, D. A., Snape, I. and Thornley, R. S.: Late Silurian and Early
1206 Devonian stratigraphy and probable strike-slip tectonics in northwestern Spitsbergen, *Geol.*
1207 *Mag.*, 134, 4, 459–479, 1997.
- 1208 Gasser, D.: The Caledonides of Greenland, Svalbard and other Arctic areas: status of research and
1209 open questions, in: *New Perspectives on the Caledonides of Scandinavia and Related Areas*,
1210 edited by: Corfu, F., Gasser, D. and Chew, D. M., *Geol. Soc., London, Spec. Publi.*, 390,
1211 93–129, 2014.
- 1212 Gee, D. G. and Moody-Stuart, M.: The base of the Old Red Sandstone in central north Haakon VII
1213 Land, Vestspitsbergen, *Polarinst. Årbok*, 1964, 57–68, 1966.
- 1214 Gee, D. G. and Pease, V.: The Neoproterozoic Timanide Orogen of eastern Baltica: introduction,
1215 in: *The Neoproterozoic Timanide Orogen of eastern Baltica*, edited by: Gee, D. G. and
1216 Pease, V., *Geol. Soc. London, Mem.*, 30, 1–3, 2004.
- 1217 Gee, D. G. and Teben'kov, A. M.: Svalbard: a fragment of the Laurentian margin, in: *The*
1218 *Neoproterozoic Timanide Orogen of eastern Baltica*, edited by: Gee, D. G. and Pease, V.,
1219 *Geol. Soc. London, Mem.*, 30, 191–206, 2004.
- 1220 Gee, D. G., Björklund, L and Stølen, L.-K.: Early Proterozoic basement in Ny Friesland–
1221 implications for the Caledonian tectonics of Svalbard, *Tectonophys.*, 231, 171–182, 1994.
- 1222 Gee, D. G., Fossen, H., Henriksen, N. and Higgins, A. K.: From the Early Paleozoic Platforms of
1223 Baltica and Laurentia to the Caledonide Orogen of Scandinavia and Greenland, *Episodes*,
1224 31, 1, 44–51, 2008.
- 1225 Gernigon, L. and Brönnner, M.: Late Palaeozoic architecture and evolution of the southwestern
1226 Barents Sea: insights from a new generation of aeromagnetic data, *J. Geol. Soc., London*,
1227 169, 449–459, 2012.
- 1228 Gernigon, L., Brönnner, M., Roberts, D., Olesen, O., Nasuti, A. and Yamasaki, T.: Crustal and basin
1229 evolution of the southwestern Barents Sea: From Caledonian orogeny to continental
1230 breakup, *Tectonics*, 33, 347–373, 2014.
- 1231 Gernigon, L., Brönnner, M., Dumais, M.-A., Gradmann, S., Grønlie, A., Nasuti, A. and Roberts, D.:
1232 Basement inheritance and salt structures in the SE Barents Sea: Insights from new potential
1233 field data, *J. Geodyn.*, 119, 82–106, 2018.



- 1234 Griffin, W. L., Nikolic, N., O'Reilly, S. Y. and Pearson, N. J.: Coupling, decoupling and
1235 metasomatism: Evolution of crust–mantle relationships beneath NW Spitsbergen, *Lithos*,
1236 149, 115–135, 2012.
- 1237 Gudlaugsson, S. T., Faleide, J. I., Johansen, S. E. and Breivik, A. J.: Late Palaeozoic structural
1238 development of the South-western Barents Sea. *Mar. Petrol. Geol.*, 15, 73–102, 1998.
- 1239 Haremo, P. and Andresen, A.: Tertiary décollements thrusting and inversion structures along
1240 Billefjorden and Lomfjorden Fault Zones, East Central Spitsbergen, in: *Structural and*
1241 *Tectonic Modelling and its Application to Petroleum Geology*, edited by: Larsen, R. M.,
1242 Brekke, H., Larsen, B. T. and Talleraas, E., Norwegian Petroleum Society (NPF) Special
1243 Publications, 1, 481–494, 1992.
- 1244 Harland, W. B.: Contribution of Spitsbergen to understanding of tectonic evolution of North
1245 Atlantic region, *AAPG Memoirs*, 12, 817–851, 1969.
- 1246 Harland, W. B. and Horsfield, W. T.: West Spitsbergen Orogen, in: *Mesozoic–Cenozoic Orogenic*
1247 *Belts, data for Orogenic Studies*, *J. Geol. Soc. London, Spec. Publi.*, 4, 747–755, 1974.
- 1248 Harland, W. B. and Kelly, S. R. A.: Eastern Svalbard Platform, in: *Geology of Svalbard*, edited by:
1249 Harland, W. B., *Geol. Soc. London, Mem.*, 17, 521 pp., 1997.
- 1250 Harland, W. B. and Wright, N. J. R.: Alternative hypothesis for the pre-Carboniferous evolution of
1251 Svalbard, *Norsk Polarinst. Skr.*, 167, 89–117, 1979.
- 1252 Harland, W. B., Cutbill, L. J., Friend, P. F., Gobbett, D. J., Holliday, D. W., Maton, P. I., Parker,
1253 J. R. and Wallis, R. H.: The Billefjorden Fault Zone, Spitsbergen – the long history of a
1254 major tectonic lineament, *Norsk Polarinst. Skr.*, 161, 1–72, 1974.
- 1255 Harland, W. B., Scott, R. A., Auckland, K. A. and Snape, I.: The Ny Friesland Orogen, Spitsbergen,
1256 *Geol. Mag.*, 129, 6, 679–708, 1992.
- 1257 Harland, W. B., Hambrey, M. J. and Waddams, P.: Vendian geology of Svalbard, *Norsk Polarinst.*
1258 *Skri.*, 193, 152 pp., 1993.
- 1259 Hassaan, M., Faleide, J. I., Gabrielsen, R. H. and Tsikalas, F.: Carboniferous graben structures,
1260 evaporite accumulations and tectonic inversion in the southeastern Norwegian Barents Sea,
1261 *Mar. Petrol. Geol.*, 112, 104038, 2020a.
- 1262 Hassaan, M., Faleide, J. I., Gabrielsen, R. H. and Tsikalas, F.: Architecture of the evaporite
1263 accumulation and salt structures dynamics in Tiddlybanken Basin, southeastern Norwegian
1264 Barents Sea, *Basin Res.*, 33, 91–117, 2020b.



- 1265 Herrevold, T., Gabrielsen, R. H. and Roberts, D.: Structural geology of the southeastern part of the
1266 Trollfjorden-Komagelva Fault Zone, Varanger Peninsula, Finnmark, North Norway,
1267 Norwegian Journal of Geology, 89, 305-325, 2009.
- 1268 Horsfield, W. T.: Glauconite schists of Caledonian age from Spitsbergen, Geol. Mag., 109, 1,
1269 29–36, 1972.
- 1270 Hurich, C. A., Smithson, S. B., Fountain, D. M. and Humphreys, M. C.: Seismic evidence of
1271 mylonite reflectivity and deep structure in the Kettle dome metamorphic core complex,
1272 Washington, Geology, 13, 577–580, 1985.
- 1273 Jakobsson, M., Mayer, L., Coackley, B., Dowdeswell, J. A., Forbes, S., Fridman, B., Hodnesdal,
1274 H., Noormets, R., Pedersen, R., Rebesco, M., Schenke, H. W., Zarayskaya, Y., Accettella,
1275 D., Armstrong, A., Anderson, R. M., Bienhoff, P., Camerlenghi, A., Church, I., Edwards,
1276 M., Gardner, J. V., Hall, J. K., Hell, B., Hestvik, O., Kristoffersen, Y., Marcussen, C.,
1277 Mohammad, R., Mosher, D., Nghiem, S. V., Pedrosa, M. T., Travaglini, P. G., and
1278 Weatherall, P.: The International Bathymetric Chart of the Arctic Ocean (IBCAO) Version
1279 3.0, Geophys. Res. Lett., 39, L12609, <https://doi.org/10.1029/2012GL052219>, 2012.
- 1280 Johansen, S. E., Ostistiy, B. K., Birkeland, Ø., Fedorovsky, Y. F., Martirosjan, V. N., Bruun
1281 Christensen, O., Cheredeev, S. I., Ignatenko, E. A. and Margulis, L. S.: Hydrocarbon
1282 potential in the Barents Sea region: play distribution and potential, in: Arctic Geology and
1283 Petroleum Potential, edited by: Vorren, T. O., Bergsager, E., Dahl-Stamnes, Ø. A., Holter,
1284 E., Johansen, B., Lie, E. and Lund, T. B., NPF Spec. Publi., 2, 273–320, Elsevier,
1285 Amsterdam, 1992.
- 1286 Johansson, Å., Larionov, A. N., Gee, D. G., Ohta, Y., Tebenkov, A. M. and Sandelin, S.:
1287 Grenvillian and Caledonian tectono-magmatic activity in northeasternmost Svalbard, in:
1288 The Neoproterozoic Timanide Orogen of Eastern Baltica, edited by: Gee, D. G. and Pease,
1289 V., Geol. Soc. London Memoirs, 30, 207–232, 2004.
- 1290 Johansson, Å., Gee, D. G., Larionov, A. N., Ohta, Y. and Tebenkov, A. M.: Grenvillian and
1291 Caledonian evolution of eastern Svalbard – a tale of two orogenies, Terra Nova, 17, 317–
1292 325, 2005.
- 1293 Kairanov, B., Escalona, A., Mordascova, A., Sliwinska, K. and Suslova, A.: Early Cretaceous
1294 tectonostratigraphy evolution of the north central Barents Sea, J. Geodyn., 119, 183–198,
1295 2018.



- 1296 Klitzke, P., Franke, D., Ehrhardt, A., Lutz, R., Reinhardt, L., Heyde, I. and Faleide, J. I.: The
1297 Palaeozoic Evolution of the Olga Basin Region, Northern Barents Sea: A Link to the
1298 Timanian Orogeny, *Geochem., Geophys., Geosy.*, 20, 614–629, 2019.
- 1299 Knudsen, C., Gee, D. G., Sherlock, S. C. and Yu, L.: Caledonian metamorphism of metasediments
1300 from Franz Josef Land, *GFF*, 141, 295–307, 2019.
- 1301 Koehl, J.-B. P.: Early Cenozoic Eureka strain partitioning and decoupling in central Spitsbergen,
1302 Svalbard, *Solid Earth*, 12, 1025–1049, 2020a.
- 1303 Koehl, J.-B. P.: Impact of Timanian thrusts on the Phanerozoic tectonic history of Svalbard,
1304 Keynote lecture, EGU General Assembly, May 3rd–8th 2020, Vienna, Austria, 2020b.
- 1305 Koehl, J.-B. P. and Muñoz-Barrera, J. M.: From widespread Mississippian to localized
1306 Pennsylvanian extension in central Spitsbergen, Svalbard, *Solid Earth*, 9, 1535–1558, 2018.
- 1307 Koehl, J.-B. P., Bergh, S. G., Henningsen, T. and Faleide, J. I.: Middle to Late Devonian–
1308 Carboniferous collapse basins on the Finnmark Platform and in the southwesternmost
1309 Nordkapp basin, SW Barents Sea, *Solid Earth*, 9, 341–372, 2018.
- 1310 Koehl, J.-B. P., Bergh, S. G., Osmundsen, P. T., Redfield, T., Indrevær, K., Lea, H. and Bergø, E.:
1311 Late Devonian–Carboniferous faulting and controlling structures and fabrics in NW
1312 Finnmark, *Norw. J. Geol.*, 99, 3, 1–40, 2019.
- 1313 Koehl, J.-B. P., Allaart, L. and Noormets, R.: Devonian–Carboniferous collapse and segmentation
1314 of the Billefjorden Trough, and Eureka inversion–overprint and strain partitioning and
1315 decoupling along inherited WNW–ESE-striking faults, in review, 2021.
- 1316 Korago, E. A., Kovaleva, G. N., Lopatin, B. G. and Orgo, V. V.: The Precambrian rocks of Novaya
1317 Zemlya, in: *The Neoproterozoic Timanide Orogen of Eastern Baltica*, edited by: Gee, D.
1318 G. and Pease, V., *Geol. Soc. London, Mem.*, 30, 135–143, 2004.
- 1319 Kosminska, K., Majka, J., Mazur, S., Krumbholz, M., Klonowska, I., Manecki, M., Czerny, J. and
1320 Dwornik, M.: Blueschist facies metamorphism in Nordenskiöld Land of west-central
1321 Svalbard, *Terra Nova*, 26, 377–386, 2014.
- 1322 Kostyuchenko, A., Sapozhnikov, R., Egorkin, A., Gee, D. G., Berzin, R. and Solodilov, L.: Crustal
1323 structure and tectonic model of northeastern Baltica, based on deep seismic and potential
1324 field data, in: *European Lithosphere Dynamics*, edited by: Gee, D. G. and Stephenson, R.
1325 A., *Geol. Soc. London Mem.*, 32, 521–539, 2006.



- 1326 Labrousse, L., Elvevold, S., Lepvrier, C. and Agard, P.: Structural analysis of high-pressure
1327 metamorphic rocks of Svalbard: Reconstructing the early stages of the Caledonian orogeny,
1328 *Tectonics*, 27, 22 pp., 2008.
- 1329 Lamar, D. L. and Douglass, D. N.: Geology of an area astride the Billefjorden Fault Zone, Northern
1330 Dicksonland, Spitsbergen, Svalbard, *Polarist. Skr.*, 197, 46 pp., 1995.
- 1331 Lamar, D. L., Reed, W. E. and Douglass, D. N.: Billefjorden fault zone, Spitsbergen: Is it part of a
1332 major Late Devonian transform?, *GSA*, 97, 1083–1088, 1986.
- 1333 Larssen, G. B., Elvebakk, G., Henriksen, L. B., Kristensen, S.-E., Nilsson, I., Samuelsberg, T. J.,
1334 Svånå, T. A., Stemmerik, L. and Worsley, D.: Upper Palaeozoic lithostratigraphy of the
1335 Southern part of the Norwegian Barents Sea, *Norges geol. unders. Bull.*, 444, 45 pp., 2005.
- 1336 Lasabuda, A., Laberg, J. S., Knutsen, S.-M. and Safronova, P.: Cenozoic tectonostratigraphy and
1337 pre-glacial erosion: A mass-balance study of the northwestern Barents Sea margin,
1338 *Norwegian Arctic, J. Geodyn.*, 119, 149–166, 2018.
- 1339 Lippard, S. J. and Prestvik, T.: Carboniferous dolerite dykes on Magerøy: new age determination
1340 and tectonic significance, *Norsk Geologisk Tidsskrift*, 77, 159-163, 1997.
- 1341 Livshits, Yu. Ya.: Tectonics of Central Vestspitsbergen, in: *Geology of Spitsbergen*, edited by:
1342 Sokolov, V. N., National Lending Library of Science and Technology, Boston Spa.,
1343 Yorkshire, UK, 59–75, 1965a.
- 1344 Livshits, Yu. Ya.: Paleogene deposits of Nordenskiöld Land, Vestspitsbergen, in: *Geology of*
1345 *Spitsbergen*, edited by: Sokolov, V. N., National Lending Library of Science and
1346 Technology, Boston Spa., Yorkshire, UK, 193–215, 1965b.
- 1347 Lopatin, B. G., Pavlov, L. G., Orgo, V. V. and Shkarubo, S. I.: Tectonic Structure of Novaya
1348 Zemlya, *Polarforschung*, 69, 131–135, 2001.
- 1349 Lorenz, H., Männik, P., Gee, D. and Proskurnin, V.: Geology of the Severnaya Zemlya Archipelao
1350 and the North Kara Terrane in the Russian high Arctic, *Int. J. Earth Sci.*, 97, 519–547, 2008.
- 1351 Lowell, J. D.: Spitsbergen tertiary Orogenic Belt and the Spitsbergen Fracture Zone, *GSA Bull.*,
1352 83, 3091–3102, 1972.
- 1353 Lyberis, N. and Manby, G.: Continental collision and lateral escape deformation in the lower and
1354 upper crust: An example from Caledonide Svalbard, *Tectonics*, 18, 1, 40–63, 1999.
- 1355 Majka, J. and Kosminska, K.: Magmatic and metamorphic events recorded within the Southwestern
1356 Basement Province of Svalbard, *Arktos*, 3:5, 2017.



- 1357 Majka, J., Mazur, S., Manecki, M., Czerny, J. and Holm, D. K.: Late Neoproterozoic amphibolite-
1358 facies metamorphism of a pre-Caledonian basement block in southwest Wedel Jarlsberg
1359 Land, Spitsbergen: new evidence from U–Th–Pb dating of monazite, *Geol. Mag.*, 145, 6,
1360 822–830, 2008.
- 1361 Majka, J., Larionov, A. N., Gee, D. G., Czerny, J. and Prsek, J.: Neoproterozoic pegmatite from
1362 Skoddefjellet, Wedel Jarlsberg Land, Spitsbergen: Additional evidence for c. 640 Ma
1363 tectonothermal event in the Caledonides of Svalbard, *Polish Polar Res.*, 33, 1–17, 2012.
- 1364 Majka, J., De’eri-Shlevin, Y., Gee, D. G., Czerny, J., Frei, D. and Ladenberger, A.: Torellian (c.
1365 640 Ma) metamorphic overprint of Tonian (c. 950 Ma) basement in the Caledonides of
1366 southwestern Svalbard, *Geol. Mag.*, 151, 4, 732–748, 2014.
- 1367 Manby, G. M. and Lyberis, N.: Tectonic evolution of the Devonian Basin of northern Spitsbergen,
1368 *Norsk Geol. Tidsskr.*, 72, 7–19, 1992.
- 1369 Manby, G. M., Lyberis, N., Chorowicz, J. and Thiedig, F.: Post-Caledonian tectonics along the
1370 Billefjorden fault zone, Svalbard, and implications for the Arctic region, *Geol. Soc. Am.
1371 Bul.*, 105, 201–216, 1994.
- 1372 Manecki, M., Holm, D. K., Czerny, J. and Lux, D.: Thermochronological evidence for late
1373 Proterozoic (Vendian) cooling in southwest Wedel Jarlsberg Land, Spitsbergen, *Geological
1374 Magazine*, 135, 63–9, 1998.
- 1375 Marelllo, L., Ebbing, J. and Gernigon, L.: Magnetic basement study in the Barents Sea from
1376 inversion and forward modelling, *Tectonophys.*, 493, 153–171, 2010.
- 1377 Marelllo, L., Ebbing, J. and Gernigon, L.: Basement inhomogeneities and crustal setting in the
1378 Barents Sea from a combined 3D gravity and magnetic model, *Geophys. J. Int.*, 193, 2,
1379 557–584, 2013.
- 1380 Mazur, S., Czerny, J., Majka, J., Manecki, M., Holm, D., Smyrak, A. and Wypych, A.: A strike-
1381 slip terrane boundary in Wedel Jarlsberg Land, Svalbard, and its bearing on correlations of
1382 SW Spitsbergen with the Pearya terrane and Timanide belt, *J. Geol. Soc. London*, 166, 529–
1383 544, 2009.
- 1384 McCann, A. J.: Deformation of the Old Red Sandstone of NW Spitsbergen; links to the Ellesmerian
1385 and Caledonian orogenies, in: *New Perspectives on the Old Red Sandstone*, edited by:
1386 Friends, P. F. and Williams, B. P. J., *Geol. Soc. London*, 180, 567–584, 2000.



- 1387 Merdith, A. S., Williams, S. E., Collins, A. S., Tetley, M. G., Mulder, J. A., Blades, M. L., Young,
1388 A., Armistead, S. E., Cannon, J., Zahirovic, S. and Müller, R. D.: Extending full-plate
1389 tectonic models into deep time: Linking the Neoproterozoic and the Phanerozoic, *Earth-*
1390 *Sci. Rev.*, 214, 103477, 2021.
- 1391 Müller, R., Klausen, T. G., Faleide, J. I., Olaussen, S., Eide, C. H. and Suslova, A.: Linking regional
1392 unconformities in the Barents Sea to compression-induced forebulge uplift at the Triassic-
1393 Jurassic transition, *Tectonophys.*, 765, 35–51, 2019.
- 1394 Murascov, L. G. and Mokin, Ju. I.: Stratigraphic subdivision of the Devonian deposits of
1395 Spitsbergen, *Polarinst. Skr.*, 167, 249–261, 1979.
- 1396 Nasuti, A., Roberts, D. and Gernigon, L.: Multiphase mafic dykes in the Caledonides of northern
1397 Finnmark revealed by a new high-resolution aeromagnetic dataset, *Norwegian Journal of*
1398 *Geology*, 95, 251–263, 2015.
- 1399 Norton, M. G., McClay, K. R. and Way, N. A.: Tectonic evolution of Devonian basins in northern
1400 Scotland and southern Norway, *Norsk Geol. Tidsskr.*, 67, 323–338, 1987.
- 1401 Oakey, G. N. and Chalmers, J. A.: A new model for the Paleogene motion of Greenland relative to
1402 North America: Plate reconstructions of the Davis Strait and Nares Strait regions between
1403 Canada and Greenland, *J. of Geophys. Res.*, 117, B10401, 2012.
- 1404 Ogata, K., Mulrooney, M. J., Braathen, A., Maher, H., Osmundsen, P. T., Anell, I., Smyrak-Sikora,
1405 A. A. and Balsamo, F.: Architecture, deformation style and petrophysical properties of
1406 growth fault systems: the Late Triassic deltaic succession of southern Edgeøya (East
1407 Svalbard), *Basin Res.*, 30, 5, 1042–1073, 2018.
- 1408 Ohta, Y., Dallmeyer, R. D. and Peucat, J. J.: Caledonian terranes in Svalbard, *GSA Spec. Paper*,
1409 230, 1–15, 1989.
- 1410 Ohta, Y., Krasil'scikov, A. A., Lepvrier, C. and Teben'kov, A. M.: Northern continuation of
1411 Caledonian high-pressure metamorphic rocks in central-western Spitsbergen, *Polar Res.*,
1412 14, 3, 303–315, 1995.
- 1413 Olovyanishnikov, V. G., Roberts, D. and Siedlecka, A.: Tectonics and Sedimentation of the
1414 Meso- to Neoproterozoic Timan-Varanger Belt along the Northeastern Margin of Baltica,
1415 *Polarforschung*, 68, 267–274, 2000.



- 1416 Osmundsen, P-T., Braathen, A., Rød, R. S. and Hynne, I. B.: Styles of normal faulting and fault-
1417 controlled sedimentation in the Triassic deposits of Eastern Svalbard, Norwegian Petroleum
1418 directorate Bulletin, 10, 61–79, 2014.
- 1419 Petersen, T. G., Thomsen, T. B., Olaussen, S. and Stemmerik, L.: Provenance shifts in an evolving
1420 Eureka foreland basin: the Tertiary Central Basin, Spitsbergen, *J. Geol. Soc., London*, 173,
1421 634–648, 2016.
- 1422 Peucat, J.-J., Ohta, Y., Gee, D. G. and Bernard-Griffiths, J.: U-Pb, Sr and Nd evidence for
1423 Grenvillian and latest Proterozoic tectonothermal activity in the Spitsbergen Caledonides,
1424 *Arctic Ocean, Lithos*, 22, 275–285, 1989.
- 1425 Phillips, T., Jackson, C. A-L., Bell, R. E., Duffy, O. B. and Fossen, H.: Reactivation of
1426 intrabasement structures during rifting: A case study from offshore southern Norway,
1427 *Journal of Structural Geology*, 91, 54–73, 2016.
- 1428 Piepjohn, K.: The Svalbardian–Ellesmerian deformation of the Old Red Sandstone and the pre-
1429 Devonian basement in NW Spitsbergen (Svalbard), in: *New Perspectives on the Old Red
1430 Sandstone*, edited by: Friend, P. F. and Williams, B. P. J., *Geol. Soc. London Spec. Publi.*,
1431 180, 585–601, 2000.
- 1432 Piepjohn, K.: von Gosen, W., Läufer, A., McClelland, W. C. and Estrada, S.: Ellesmerian and
1433 Eureka fault tectonics at the northern margin of Ellesmere Island (Canadian High Arctic),
1434 *Z. Dt. Ges. Geowiss.*, 164, 1, 81–105, 2013.
- 1435 Piepjohn, K., Dallmann, W. K. and Elvevold, S.: The Lomfjorden Fault Zone in eastern Spitsbergen
1436 (Svalbard), in: *Circum-Arctic Structural Events: Tectonic Evolution of the Arctic Margins
1437 and Trans-Arctic Links with Adjacent Orogens*, edited by: Piepjohn, K., Strauss, J. V.,
1438 Reinhardt, L. and McClelland, W. C., *GSA Spec. Paper*, 541, 95–130, 2019.
- 1439 Ramsay, J. G.: Interference Patterns Produced by the Superposition of Folds of Similar Type, *J.*
1440 *Geol.*, 70, 4, 466–481, 1962.
- 1441 Rice, A. H. N.: Restoration of the External Caledonides, Finnmark, North Norway, in: *New
1442 Perspectives on the Caledonides of Scandinavia and Related Areas*, Corfu, F., Gasser, D.
1443 and Chew, D. M. (eds), *Geological Society, London, Special Publications*, 390, 271–299,
1444 2014.
- 1445 Roberts, D.: Tectonic Deformation in the Barents Sea Region of Varanger Peninsula, Finnmark,
1446 *Norges geol. unders.*, 282, 1–39, 1972.



- 1447 Roberts, D. and Olovyanishshnikov, V.: Structural and tectonic development of the Timanide
1448 orogeny, in: *The Neoproterozoic Timanide Orogen of Eastern Baltica*, edited by: Gee, D.
1449 G. and Pease, V., *Geol. Soc. London, Mem.*, 30, 47–57, 2004.
- 1450 Roberts, D. and Siedlecka, A.: Timanian orogenic deformation along the northeastern margin of
1451 Baltica, Northwest Russia and Northeast Norway, and Avalonian-Cadomian connections,
1452 *Tectonophysics*, 352, 1r69-184, 2002.
- 1453 Roberts, D. and Williams, G. D.: *Berggrunnskart Kjøllefjord 2236 IV, M 1:50.000, foreløpig*
1454 *utgave, Norges geol. unders.*, 2013.
- 1455 Roberts, D., Mitchell, J. G. and Andersen, T. B.: A post-Caledonian dyke from Magerøy North
1456 Norway: age and geochemistry, *Norwegian Journal of Geology*, 71, 289-294, 1991.
- 1457 Rosa, D., Majka, J., Thrane, K. and Guarnieri, P.: Evidence for Timanian-age basement rocks in
1458 North Greenland as documented through U–Pb zircon dating of igneous xenoliths from the
1459 Midtkap volcanic centers, *Precambrian Res.*, 275, 394–405, 2016.
- 1460 Schiffer, C., Doré, A. G., Foulger, G. R., Franke, D., Geoffroy, L., Gernigon, L., Holdsworth, B.,
1461 Kuszniir, N., Lundin, E., McCaffrey, K., Peace, A. L., Petersen, K. D., Phillips, T. B.,
1462 Stephenson, R., Stoker, M. S. and Welford, J. K.: Structural inheritance in the North
1463 Atlantic, *Earth-Science Reviews*, 206, 102975, 2020.
- 1464 Senger, K., Roy, S., Braathen, A., Buckley, S., Bælum, K., Gernigon, L., Mjelde, R., Noormets,
1465 R., Ogata, K., Olaussen, S., Planke, S., Ruud, B. O. and Tveranger, J.: Geometries of
1466 doleritic intrusions in central Spitsbergen, Svalbard: an integrated study of an onshore-
1467 offshore magmatic province with applications to CO₂ sequestration, *Norw. J. Geol.*, 93,
1468 143–166, 2013.
- 1469 Siedlecka, A.: Late Precambrian Stratigraphy and Structure of the North-Eastern Margin of the
1470 Fennoscandian Shield (East Finnmark – Timan Region), *Nor. geol. unders.*, 316, 313-348,
1471 1975.
- 1472 Siedlecka, A. and Roberts, D.: Report from a visit to the Komi Branch of the Russian Academy of
1473 Sciences in Syktyvkar, Russia, and from fieldwork in the central Timans, August 1995,
1474 *Norges geol. unders. report*, 95.149, 32 pp., 1995.
- 1475 Siedlecka, A. and Siedlecki, S.: Some new aspects of the geology of Varanger peninsula (Northern
1476 Norway), *Nor. geol. unders.*, 247, 288-306, 1967.



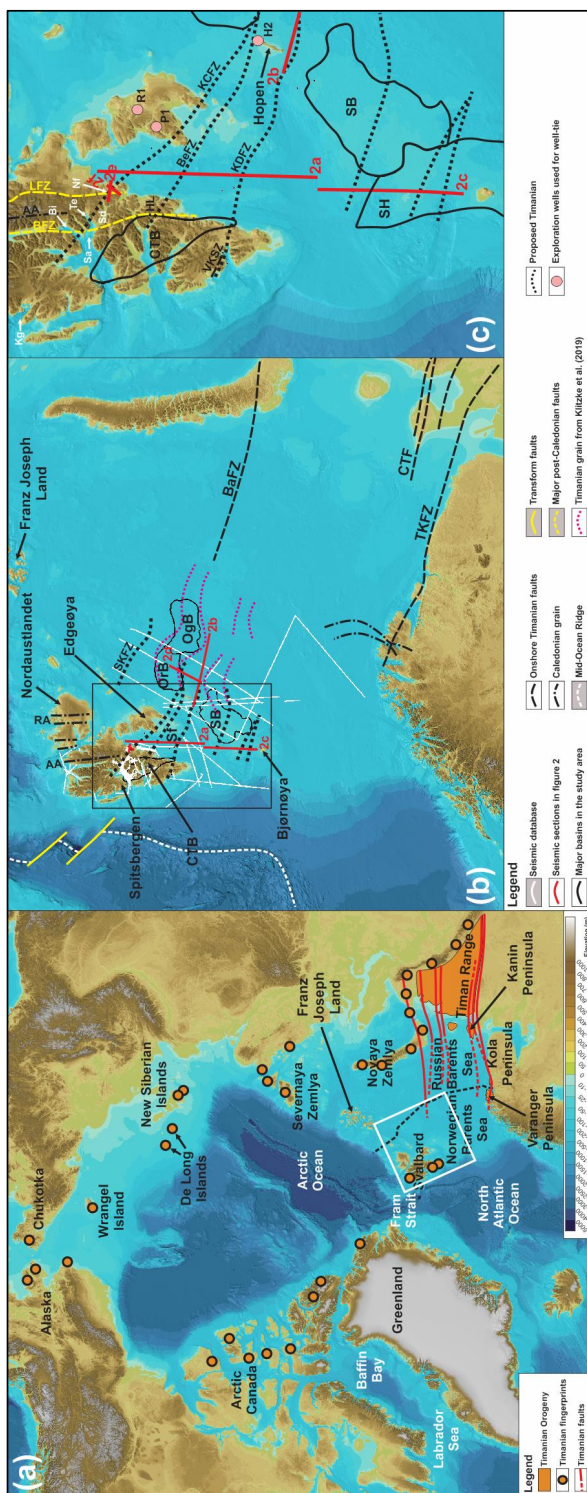
- 1477 Siedlecka, A. and Siedlecki, S.: Late Precambrian sedimentary rocks of the Tanafjord–
1478 Varangerfjord region of Varanger Peninsula, Northern Norway, in: *The Caledonian*
1479 *Geology of Northern Norway*, edited by: Roberts, D. and Gustavson, M., Norges geol.
1480 unders., 269, 246–294, 1971.
- 1481 Smyrak-Sikora, A., Osmundsen, P. T., Braathen, A., Ogata, K., Anell, I., Mulrooney, M. J. and
1482 Zuchuat, V.: Architecture of growth basins in a tidally influenced, prodelta to delta-front
1483 setting: The Triassic succession of Kvalpynten, East Svalbard, *Basin Research*, 32, 5, 959–
1484 988, 2020.
- 1485 Stouge, S., Christiansen, J. L. and Holmer, L. E.: Lower Palaeozoic stratigraphy of
1486 Murchisonfjorden and Sparreneset, Nordaustlandet, Svalbard, *Geografiska Annaler: Series*
1487 *A, Physical Geography*, 93, 209–226, 2011.
- 1488 Sturt, B. A., Pringle, I. R. and Ramsay, D. M.: The Finnmarkian phase of the Caledonian Orogeny,
1489 *J. Geol., Soc., London*, 135, 597–610, 1978.
- 1490 Thiede, J., Pfirman, S., Schenke, H.-W. and Reil, W.: Bathymetry of Molloy Deep: Fram Strait
1491 Between Svalbard and Greenland, *Mar. Geophys. Res.*, 12, 197–214, 1990.
- 1492 Tonstad, S. A.: The Late Paleozoic development of the Ottar basin from seismic 3D interpretation,
1493 Master's Thesis, University of Tromsø, Tromsø, Norway, 135 pp., 2018.
- 1494 Torsvik, T. H. and Trench, A.: The Ordovician history of the Iapetus Ocean in Britain: new
1495 palaeomagnetic constraints, *J. Geol. Soc., London*, 148, 423–425, 1991.
- 1496 Torsvik, T. H., Burke, K., Steinberger, B., Webb, S. J. and Ashwal, L. D.: Diamond sampled by
1497 plumes from the core–mantle boundary, *Nature Lett.*, 466, 352–355, 2010.
- 1498 Townsend, C.: Thrust transport directions and thrust sheet restoration in the Caledonides of
1499 Finnmark, North Norway, *J. Structural Geol.*, 9, 3, 345–352, 1987.
- 1500 Vernikovsky, V. A., Metelkin, D. V., Vernikovskaya, A. E., Matushkin, N. Yu., Lobkovsky, L. I.
1501 and Shipilov, E. V.: Early evolution stage of the arctic margins (Neoproterozoic-Paleozoic)
1502 and plate reconstructions, *ICAM VI Proceedings*, May 2011, Fairbanks, Alaska, USA, 265–
1503 285, 2011.
- 1504 Von Gosen, W. and Piepjohn, K.: Polyphase Deformation in the Eastern Hornsund Area, *Geol. Jb.*,
1505 B91, 291–312, 2001.
- 1506 Witt-Nilsson, P., Gee, D. G. and Hellman, F. J.: Tectonostratigraphy of the Caledonian Atomfjella
1507 Antiform of northern Ny Friesland, Svalbard, *Norsk Geol. Tidsskr.*, 78, 67–80, 1998.



1508 Worsley, D., Agdestein, T., Gjelberg, J. G., Kirkemo, K., Mørk, A., Nilsson, I., Olaussen, S., Steel,
1509 R. J. and Stemmerik, L.: The geological evolution of Bjørnøya, Arctic Norway:
1510 implications for the Barents Shelf, Norsk Geol. Tidsskr., 81, 195–234, 2001.
1511 Ziegler, P. A.: Evolution of the Arctic–North Atlantic and the Western Tethys, AAPG Mem. 43,
1512 1988.
1513

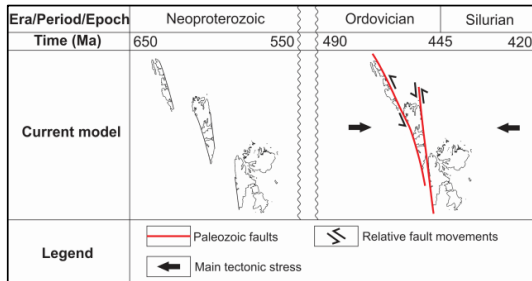


1514 **Figures**



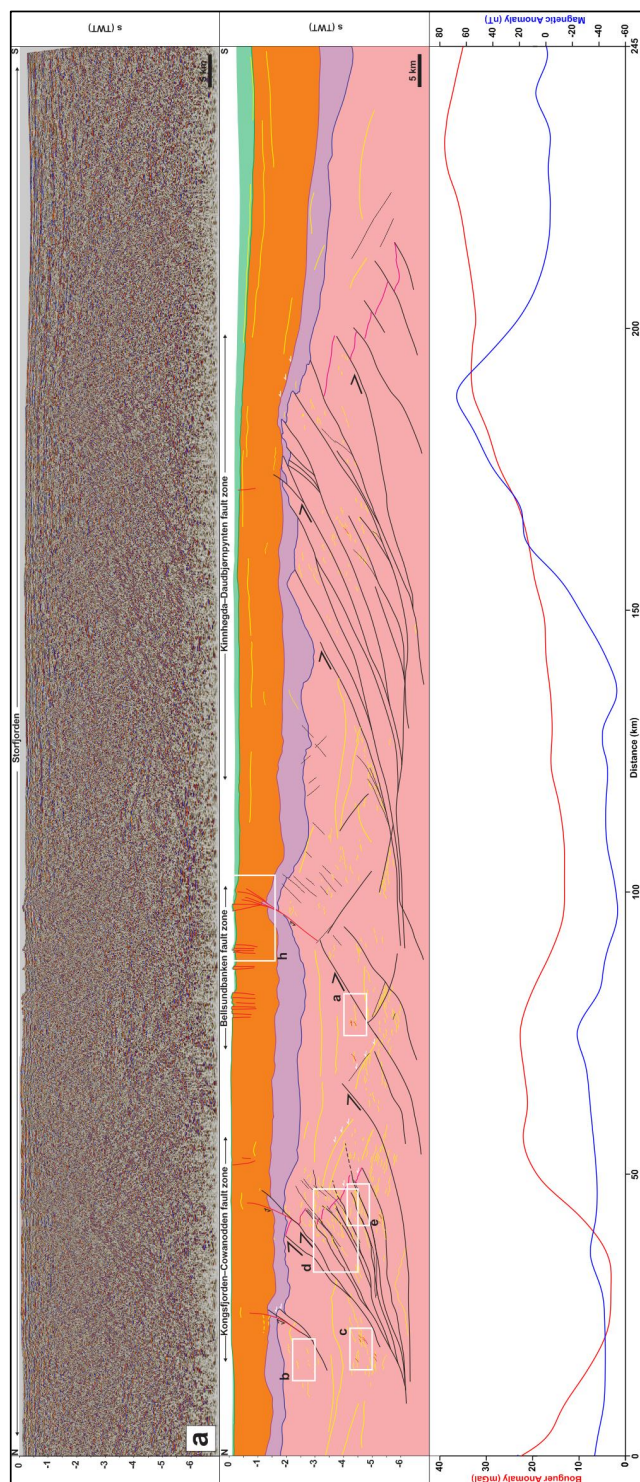


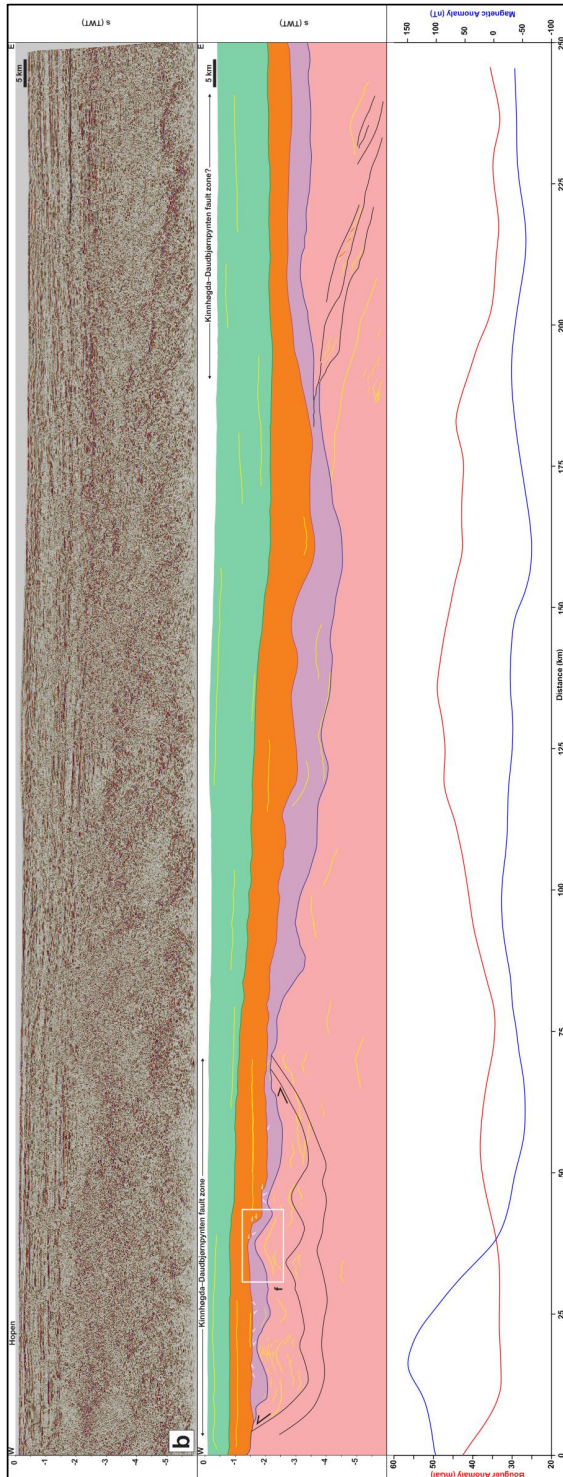
1516 **Figure 1: (a) Overview map showing the Timanian belt in Russia and Norway, and occurrences of Timanian fingerprints**
1517 **throughout the Arctic; (b) Regional map of Svalbard and the Barents Sea the main geological elements and the seismic**
1518 **database used in the present study. The location of (b) is shown as a white frame in (a); (c) Zoom in the northern Norwegian**
1519 **Barents Sea and Svalbard showing the main faults and basins in the study area, and the proposed Timanian structures. The**
1520 **location of (c) is shown as a black frame in (b). The location of the Raddedalen-1 well is from Smyrak-Sikora et al. (2020).**
1521 **Topography and bathymetry are from Jakobsson et al. (2012). Abbreviations: AA: Atomfjella Antiform; BaFZ: Baidaratsky**
1522 **fault zone; BeFZ: Bellsundbanken fault zone; BFZ: Billefjorden Fault Zone; Bi: Billefjorden; CTB: Central Tertiary Basin;**
1523 **HL: Heer Land; H2: Hopen-2; KCFZ: Kongsfjorden–Cowanodden fault zone; KDFZ: Kinnhøgda–Daudbjørnpynnten fault**
1524 **zone; Kg: Kongsfjorden; LFZ: Lomfjorden Fault Zone; Nf: Nordmannsfonna; OgB: Olga Basin; OrB: Ora Basin; P1:**
1525 **Plurdalen-1; RA: Rijpdalen Anticline; R1: Raddedalen-1; Sa: Sassenfjorden; SB: Sørkapp Basin; Sf: Storfjorden; SH:**
1526 **Stappen High; SKFZ: Steiløya–Krylen fault zone; Te: Tempelfjorden; TKFZ: Trollfjorden–Komagelva Fault Zone; VKSZ:**
1527 **Vimsodden–Kosibapasset Shear Zone.**

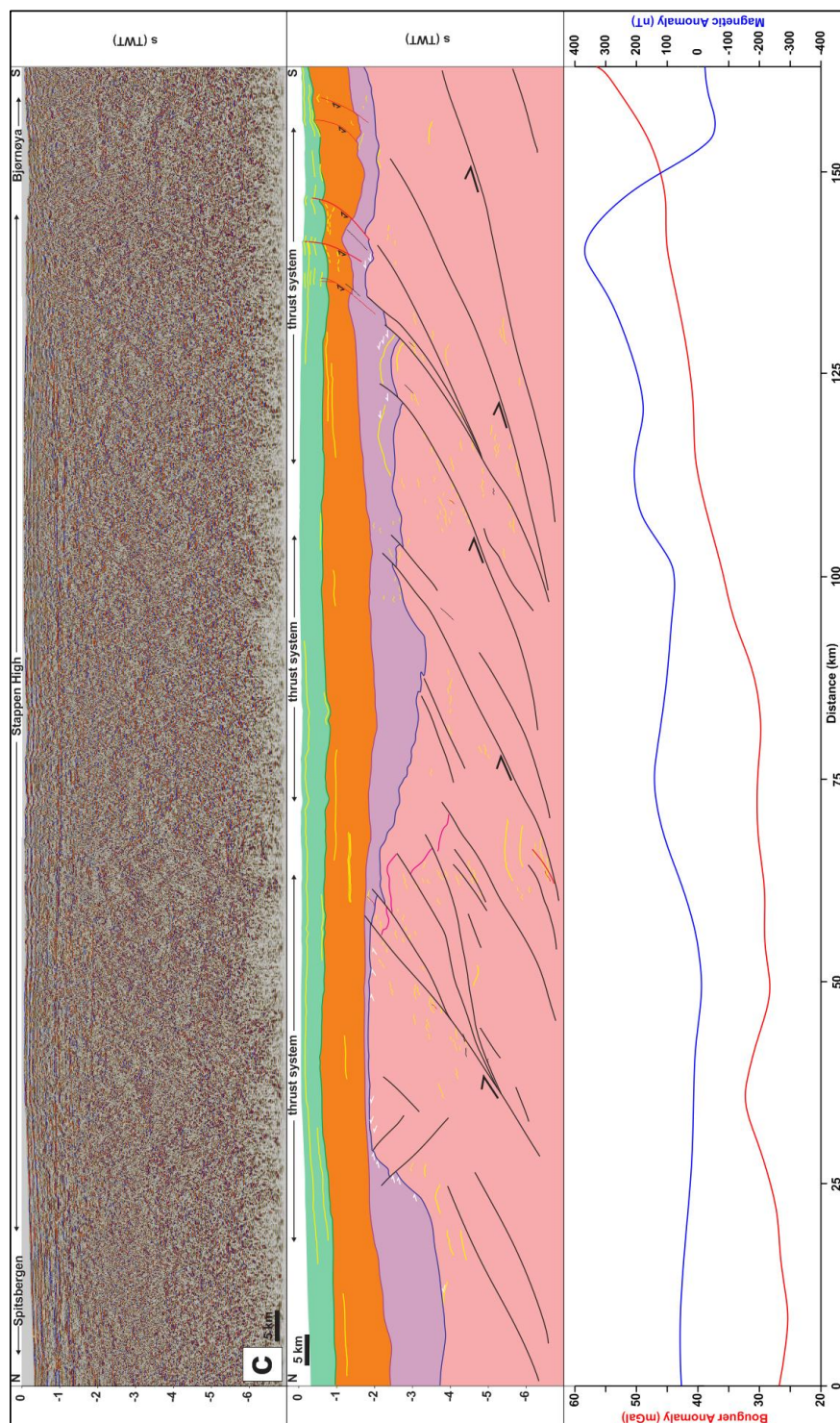


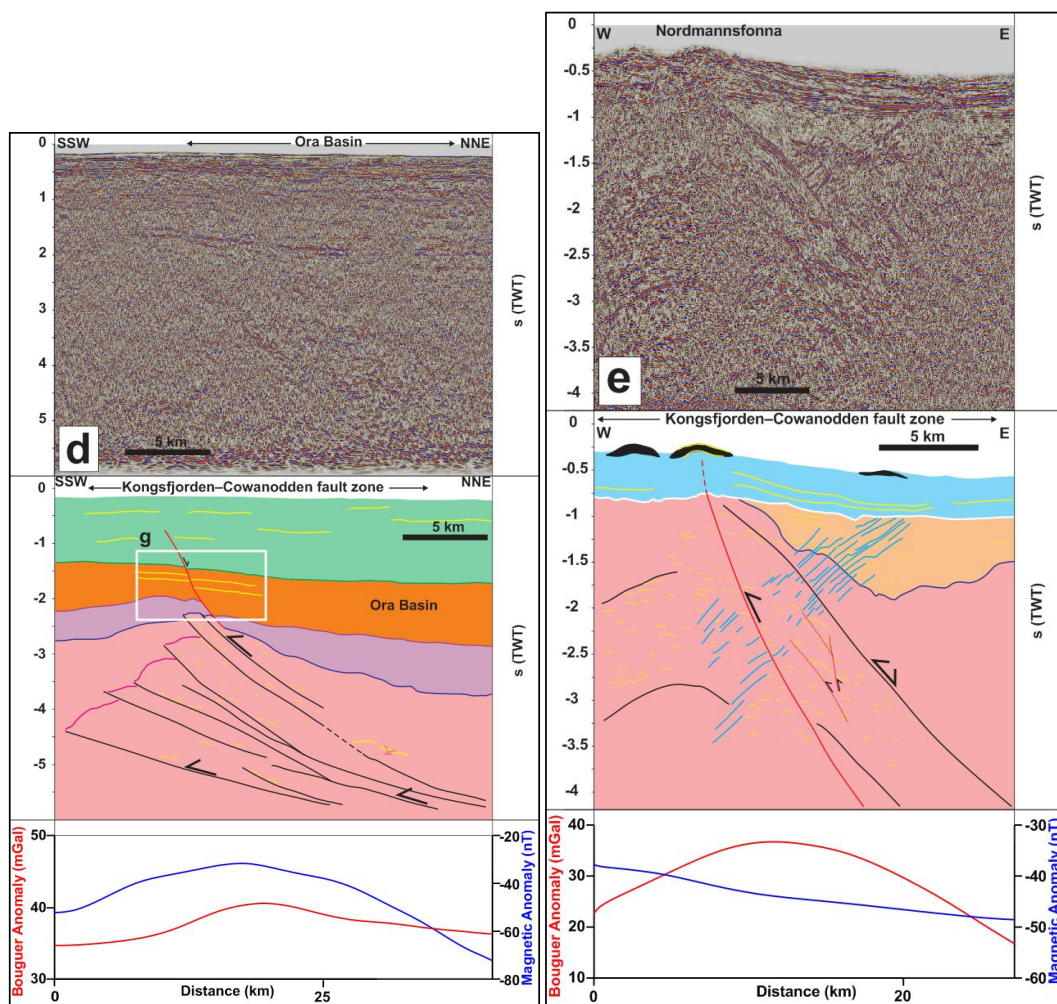
1528

1529 **Figure 2: Paleogeographic reconstruction of the Svalbard Archipelago in the latest Neoproterozoic during the Timanian**
 1530 **Orogeny and in the early–mid Paleozoic during the Caledonian Orogeny according to previous models (e.g., Harland, 1969;**
 1531 **Labrousse et al., 2008).**

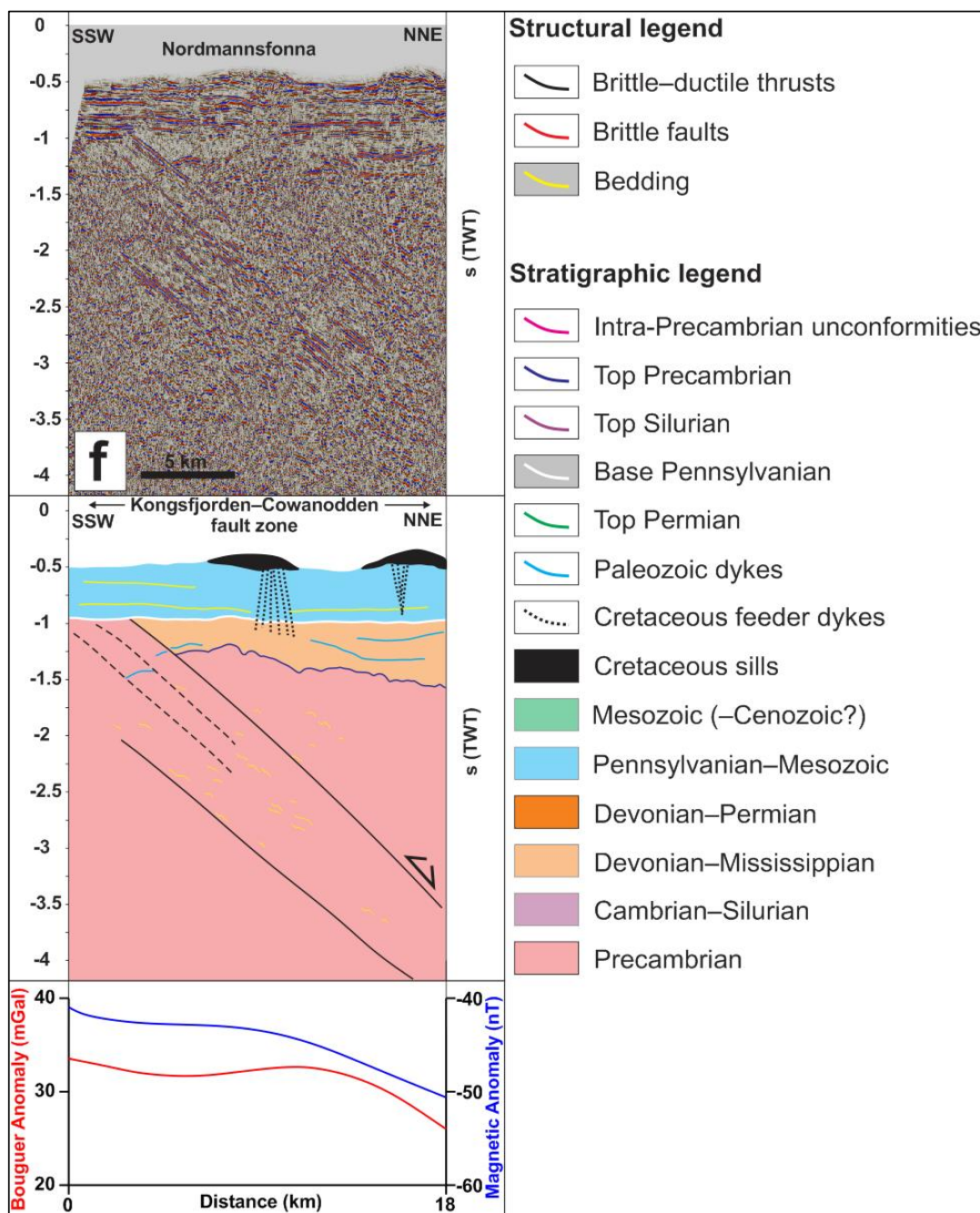








1535



1536

1537

1538

1539

1540

1541

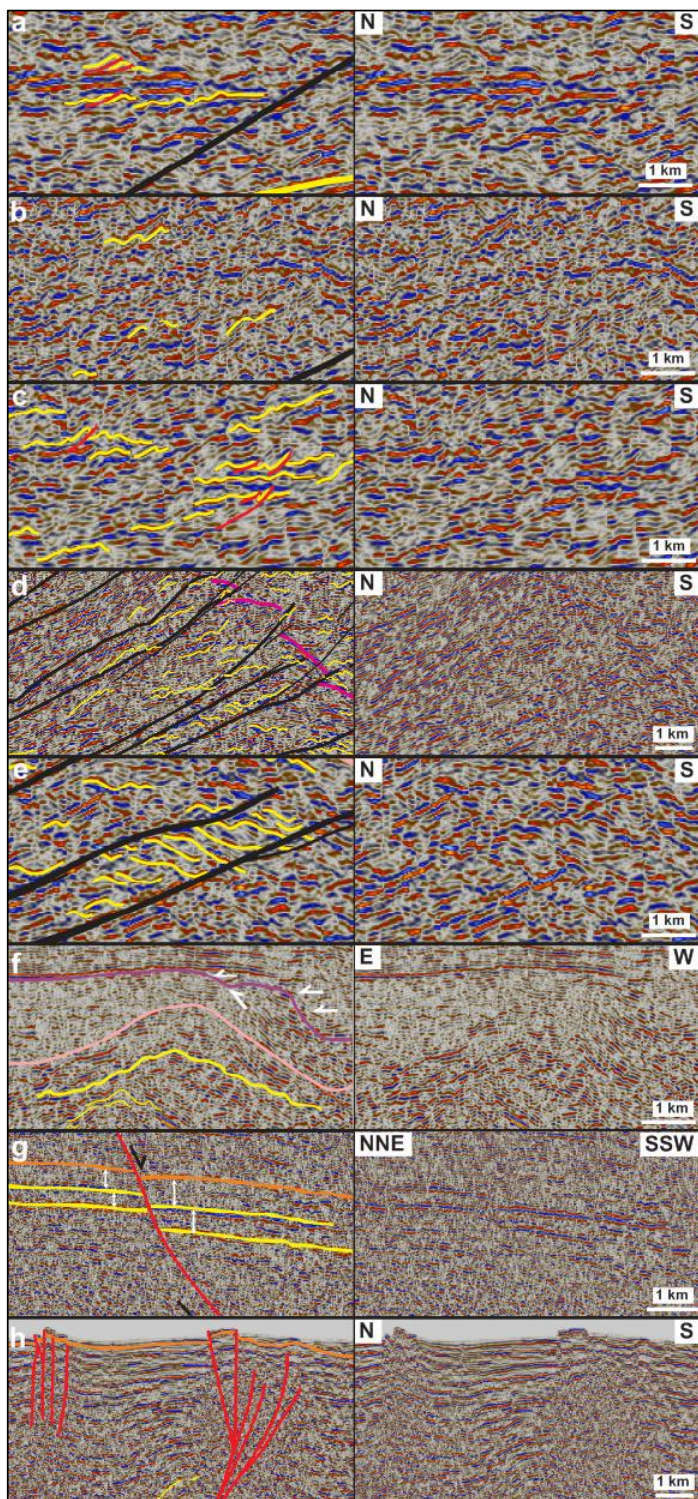
1542

Figure 3: Interpreted seismic profiles and associated potential field data (a) in Storfjorden, (b) south of Hopen, (c) on the Stappen High in the northwestern Norwegian Barents Sea between Spitsbergen and Bjørnøya, (d) on the southern flank of the Ora Basin in the northeastern Norwegian Barents Sea, and (e and f) in Nordmannsonna in eastern Spitsbergen. The seismic profiles show top-SSW Timanian thrusts that were reactivated and overprinted during subsequent tectonic events such as Caledonian contraction, Devonian–Carboniferous late–post Caledonian collapse and rifting, Eureka contraction, and present-day contraction. Profiles (e) and (f) also show Paleozoic and Cretaceous intrusions. The white frames show the



1543 location of zoomed-in portions of the profiles displayed in Figure 4. Potential field data below the seismic profiles include
1544 Bouguer anomaly (red lines) and magnetic anomaly (blue lines). The potential field data show consistently high gravimetric
1545 anomalies and partial correlation with high magnetism towards the footwall of each major thrust systems (i.e., towards
1546 thickened portions of the crust).

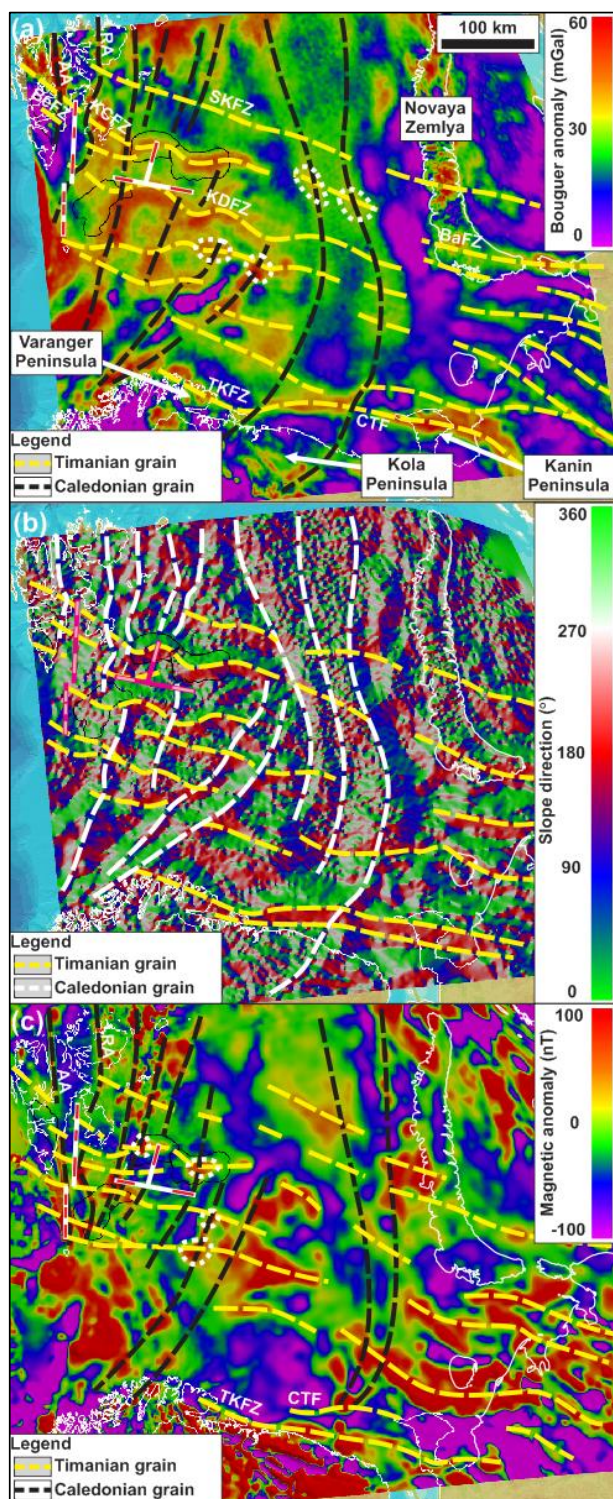
1547





1549 **Figure 4: Zooms in seismic profiles shown in Figure 3 showing (a) upright fold structures, (b) SSW-verging folds and (c)**
1550 **top-SSW minor thrusts in Precambrian–lower Paleozoic (meta-) sedimentary basement rocks, (d) SSW-verging folds and**
1551 **NNE-dipping mylonitic shear zones within a major thrust that offsets major basement unconformities (fuchsia lines) top-**
1552 **SSW, (e) duplex structures within a major top-SSW thrust, (f) a N–S- to NNE–SSW-trending, 5–15 kilometers wide,**
1553 **symmetrical , upright macro-fold and associated, kilometer- to hundreds of meter-scale, parasitic macro- to meso-folds, (g)**
1554 **syn-tectonic thickening in Devonian–Carboniferous (–Permian?) sedimentary strata offset down-NNE by a normal fault**
1555 **that merges with a thick mylonitic shear zone at depth, and (h) recent–ongoing reverse offsets of the seafloor reflection by**
1556 **multiple, inverted, NNE-dipping normal faults in Storfjorden. See Figure 3 for location of each zoom and for legend.**

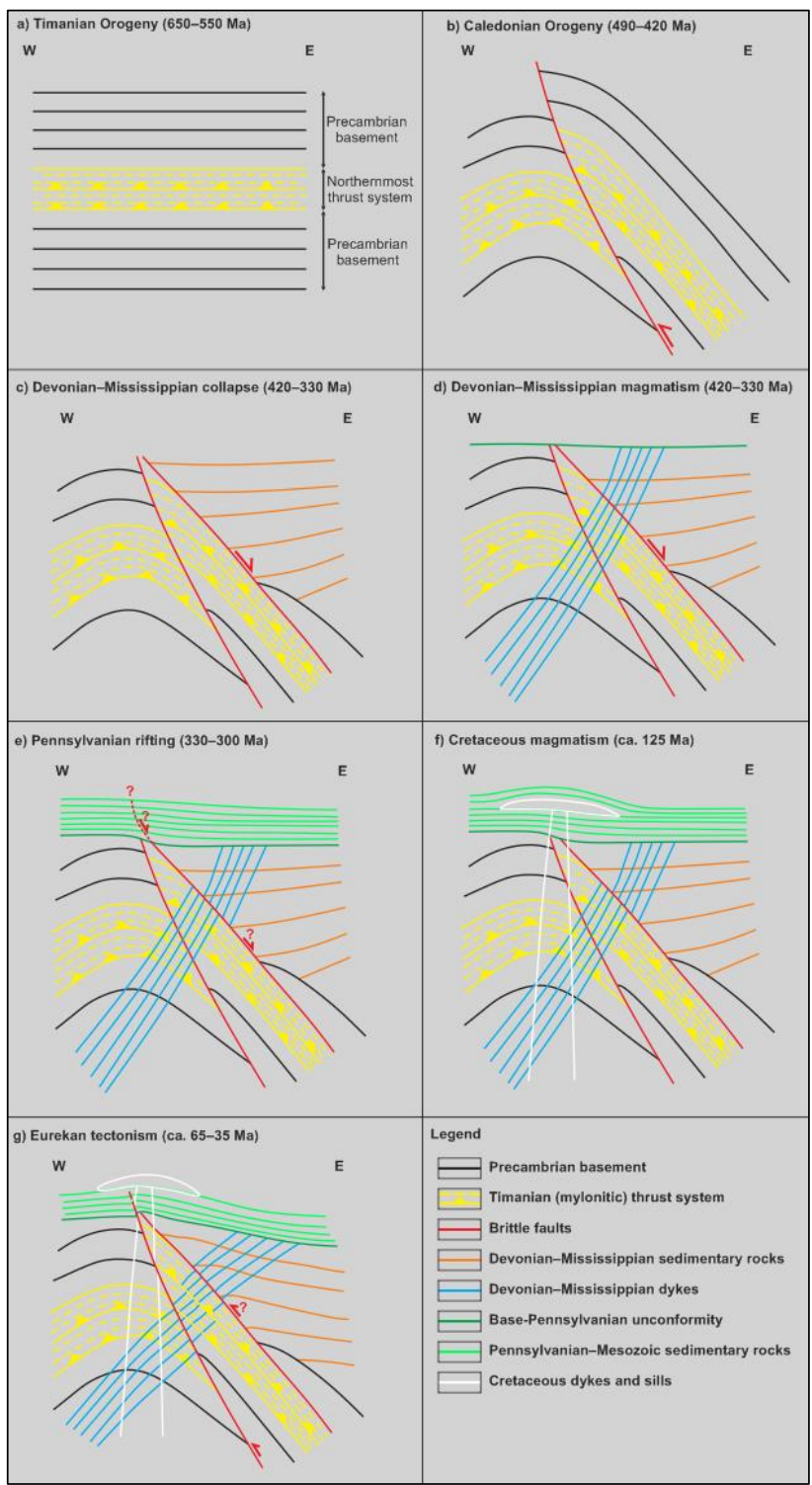
1557





1559 **Figure 5: Gravimetric (a and b) and magnetic (c) anomaly maps over the Barents Sea and adjacent onshore areas in Russia,**
1560 **Norway and Svalbard showing E–W- to NW–SE-trending anomalies (dashed yellow lines) that correlate with the proposed**
1561 **NNE-dipping Timanian thrust systems in Svalbard and the northern Norwegian Barents Sea. Note the high obliquity of E–**
1562 **W- to NW–SE-trending Timanian grain with NE–SW- to N–S-trending Caledonian grain (dashed black/white lines). Note**
1563 **that dashed lines in (a) and (c) denote high gravimetric and magnetic anomalies. Also notice the oval-shaped high**
1564 **gravimetric and magnetic anomalies (dotted white lines) at the intersection of WNW–ESE- and N–S- to NNE–SSW-trending**
1565 **anomalies in (a) and (c) resulting from the interaction of the two (Timanian and Caledonian) thrust and fold trends. The**
1566 **location of seismic profiles presented in Figure 3a–d are shown as thick white lines in (a) and (c) and as fuchsia lines in (b).**
1567 **Within these thick white and fuchsia lines, the location and extent of thrust systems evidenced on seismic data (Figure 3) is**
1568 **shown in white in (a) and (c) and in pink in (b). For the E–W-trending seismic profile shown in Figure 3b, this implies that**
1569 **the red and pink lines represent N–S-trending synclines. Abbreviations: AA: Atomfjella Antiform; BaFZ: Baidaratsky fault**
1570 **zone; BeFZ: Bellsundbanken fault zone; CTF: Central Timan Fault; KCFZ: Kongsfjorden–Cowanodden fault zone; KDFZ:**
1571 **Kinnhøgda–Daudbjørnpynten fault zone; RA: Rjipdalen Anticline; SKFZ: Steiløya–Krylen fault zone; TKFZ:**
1572 **Trollfjorden–Komagelva Fault Zone.**

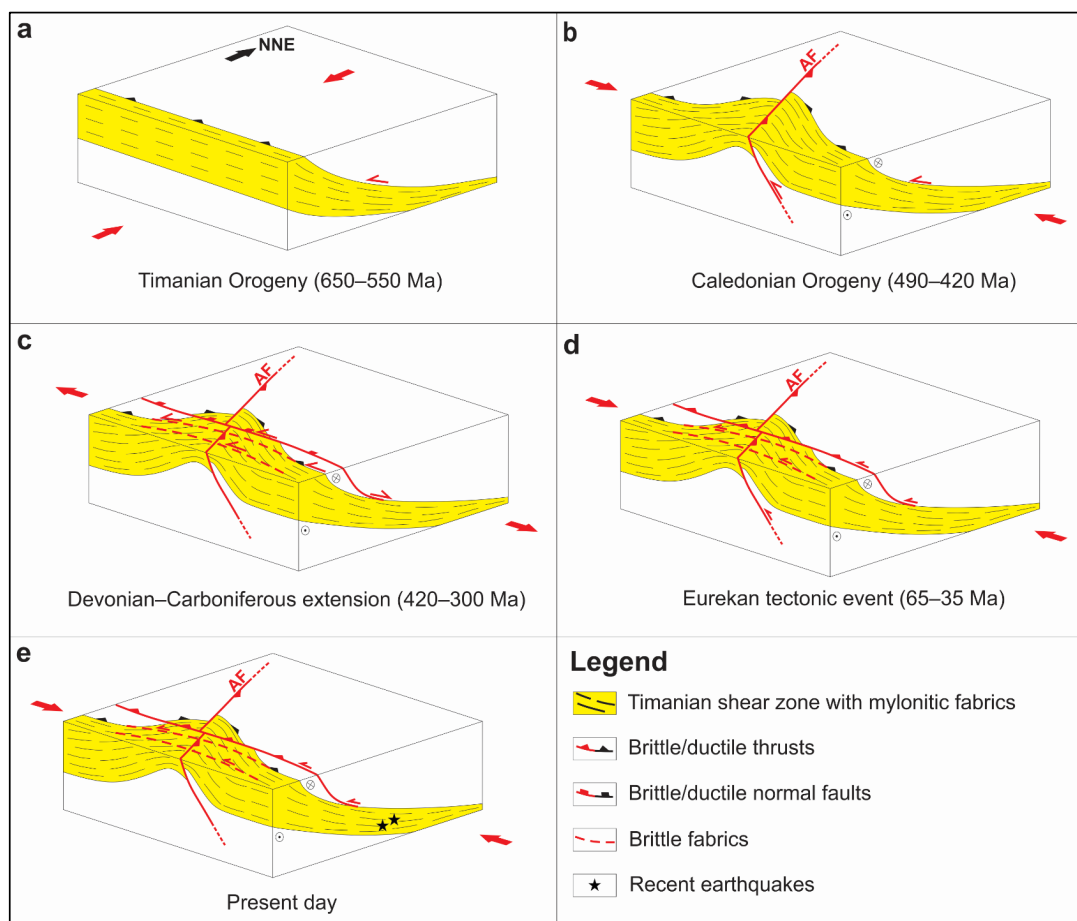
1573





1575 **Figure 6: Sketches showing a possible reconstruction of the tectonic history of the E–W seismic profile in Nordmannsfonna**
1576 **shown in Figure 3e. (a) Formation of a NNE-dipping, mylonitic thrust system (Kongsfjorden–Cowanodden fault zone)**
1577 **within Precambrian basement rocks during the Timanian Orogeny in the latest Neoproterozoic. The NNE-dipping**
1578 **Kongsfjorden–Cowanodden fault zone appears near horizontal on the E–W transect; (b) Top-west thrusting along the east-**
1579 **dipping Agardhbukta Fault and folding of the Kongsfjorden–Cowanodden fault zone into a broad, moderately NNE-**
1580 **plunging anticline during the Caledonian Orogeny; (c) Inversion of the Kongsfjorden–Cowanodden fault zone along the**
1581 **eastern flank of the Caledonian anticline and deposition of thickened, gently west-dipping, syn-tectonic, Devonian (–**
1582 **Mississippian?) sedimentary strata during post-Caledonian collapse-related extension; (d) Intrusion of Precambrian**
1583 **basement and Devonian (–Mississippian?) sedimentary rocks by steeply west-dipping dykes in the Devonian–Mississippian;**
1584 **(e) Regional erosion in the mid-Carboniferous (latest Mississippian) and deposition of Pennsylvanian sedimentary strata,**
1585 **possibly along a high-angle brittle splay of the inverted portion of the Kongsfjorden–Cowanodden fault zone during rift-**
1586 **related extension; (f) Deposition of Mesozoic sedimentary strata and intrusion of Cretaceous dolerite dykes and sills; (g)**
1587 **Erosion of Pennsylvanian–Mesozoic strata and reactivation of the Kongsfjorden–Cowanodden fault zone and Agardhbukta**
1588 **Fault with minor reverse movements in the early Cenozoic during the Eurekan tectonic event as shown by mild folding and**
1589 **offset of overlying post-Caledonian sedimentary strata, dykes and Base-Pennsylvanian unconformity. Also note the back-**
1590 **tilting (i.e., clockwise rotation) of Devonian–Mississippian dykes in the hanging wall of the Agardhbukta Fault and of the**
1591 **Kongsfjorden–Cowanodden fault zone.**

1592



1593

1594

1595

1596

1597

1598

1599

1600

1601

1602

1603

Figure 7: Tectonic evolution of Timanian thrust systems in eastern Spitsbergen, Storfjorden and the northwestern Norwegian Barents Sea including (a) top-SSW thrusting during the Timanian Orogeny, (b) reactivation as oblique-slip sinistral-reverse thrusts and offset by top-west brittle thrust overprints (e.g., Agardhbukta Fault – AF) under E–W contraction during the Caledonian Orogeny, (c) reactivation as low-angle, brittle–ductile, normal–sinistral extensional detachments and overprinting by high-angle normal–sinistral brittle faults during Devonian–Carboniferous, late–post-Caledonian extensional collapse and rifting, (d) reactivation as brittle–ductile sinistral–reverse thrusts, overprinting by high-angle sinistral–reverse brittle thrusts, and mild offset by reactivated top-west thrusts (e.g., Agardhbukta Fault – AF) during E–W Eurekan contraction, and (e) renewed, recent–ongoing, sinistral–reverse reactivation and overprinting possibly due to ongoing magma extrusion and transform faulting (ridge-push?) in the Fram Strait.